Energy & Buildings 357 (2026) 117104

Contents lists available at ScienceDirect

Energy & Buildings

journal homepage: www.elsevier.com/locate/enb

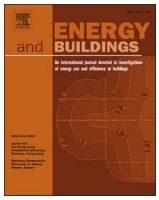

Bio-jaali: Reimagining vernacular passive cooling screens with mycelium-based composites☆

Kumar Biswajit Debnath [a,c,*], Natalia Pynirtzi [a,b], Jane Scott [a], Colin Davie [b], Ben Bridgens [a]

[a] Hub for Biotechnology in the Built Environment, School of Architecture, Planning and Landscape, Newcastle University, Newcastle Upon Tyne NE1 7RU, United Kingdom
[b] School of Engineering, Newcastle University, Newcastle Upon Tyne NE1 7RU, United Kingdom
[c] School of Architecture, University of Technology Sydney, Sydney, Australia

ARTICLE INFO

Keywords:
Mycelium-based composite
Jaali
Cooling demand reduction
Passive building skin
Climate-responsive façade

ABSTRACT

Climate change and severe urban heat stress in South Asian megacities are driving an amplified reliance on energy-intensive air conditioning, necessitating urgent low-carbon cooling solutions. This study addresses this challenge by reinterpreting the traditional jaali, a perforated passive-cooling screen, using mycelium-based composites (MBCs) to create a novel, climate-responsive, low-carbon façade system: bio-jaali. We assessed the performance of the bio-jaali through a holistic approach, combining historical climate data analysis (New Delhi, 1991–2019), dynamic building energy simulations, and laboratory bio-fabrication and hygrothermal testing. This integrated methodology is a key achievement, bridging materials science with dynamic simulation to improve building-scale performance. The climate analysis revealed a 60% increase in 'danger-level' heat-stress hours over the 28 years. Dynamic simulation results showed that replacing the conventional sandstone jaali with the bio-jaali yielded substantial thermal benefits: a 3.5°C (10%) reduction in the annual average indoor operative temperature and a drop in peak summer indoor temperatures by up to 14.8°C. Consequently, the annual cooling energy demand was lowered by 50.4%. Furthermore, laboratory cyclic humidity tests demonstrated the MBCs' potential for evaporative cooling, confirming they remained dimensionally stable (<3% change) while absorbing up to 17.2% moisture. The bio-jaali is highlighted as a culturally rooted, bio-based solution that significantly reduces reliance on active cooling. This research contributes new knowledge on the building-scale performance, climate adaptability, and cyclic hygrothermal stability of MBC facades. We position the bio-jaali as a robust prototype for integrating passive and adaptive thermal regulation, advancing circular construction practices for sustainable architecture in heat-stressed urban environments.

1. Introduction

Ten of the 33 global megacities [1] with populations exceeding 10 million are in South Asia. The United Nations projects that New Delhi will soon become the largest megacity worldwide, with Dhaka and Mumbai also likely to rank among the top ten by 2030, bringing the total to 43 megacities [1]. As climate change intensifies, extreme heatwaves are becoming a regular occurrence in South Asia [2], posing a significant challenge for the billions of residents of these megacities [3]. The health impacts of such heat exposure—including heat exhaustion, cramps, heat stroke, and potentially fatal outcomes—underscore the urgency of this issue [4]. In response, many people turn to air conditioning (A/C) for comfort and survival, leading to a substantial increase in electricity demand for cooling solutions [5,6]. For instance, India is projected to have 240 million air conditioning (A/C) units by 2030, a significant increase from 21.8 million in 2017 [7], and is expected to reach 1.2 billion units by 2050 [8]. To address these challenges constructively, it is essential to innovate building design, focusing on strategies that reduce and/or optimise reliance on energy-intensive cooling systems [9–11]. By incorporating passive cooling techniques and enhancing resilience to extreme heat events, we can create healthier, more sustainable living environments for future generations.

A range of innovative passive building skins has been developed for different climates. In South Asia, the most widely explored systems include double-skin facades, solar chimneys, and trombe walls [12,13]. Double-skin facades can offer practical thermal and acoustic benefits in

☆ This article is part of a special issue entitled: 'NBS for Climate Change' published in Energy & Buildings.
* Corresponding author at: School of Architecture, University of Technology Sydney, Sydney, Australia.

https://doi.org/10.1016/j.enbuild.2026.117104
Received 30 September 2025; Received in revised form 8 January 2026; Accepted 31 January 2026
Available online 5 February 2026

new, modern office buildings; however, they are costly, difficult to retrofit, and generally unsuitable for residential applications due to privacy, cultural, and aesthetic concerns. Solar chimneys and Trombe walls, inspired by vernacular techniques [14], offer more adaptable options for houses; however, their reliance on orientation, solar availability, and significant space requirements limits their broader application in dense urban contexts [15,16]. More recently, adaptive, intelligent, and smart building skins have been developed to enable façades to function as living systems, capable of regulating airflow and heat transfer through centralised or localised control [17–20]. Among the advanced materials supporting such systems, phase change materials (PCMs) are utilised for thermal energy storage. Electrochromic glazing allows for the modulation of daylight and solar gain, while thermochromic coatings adjust their reflectance with temperature [21–23]. While these technologies enhance environmental responsiveness, they often involve high embodied energy in production. Smart systems further depend on rare-earth metals, making them resource-intensive and less sustainable for large-scale adoption, as they are usually extracted through labour exploitation and harmful mining practices and are prone to geopolitical stressors. This pressing pursuit of low-carbon alternatives has driven extensive research into truly sustainable, bio-based materials. Solutions like Hempcrete [24] and earthen materials [25] are increasingly valued for their low embodied carbon, thermal mass, and superior hygroscopic properties that actively regulate indoor humidity and temperature. This trend validates the exploration of novel bio-composites [26–28] and metamaterials [29] that can integrate these material advantages.

This study aimed to redesign the traditional architectural element known as 'jaali' [30] —a predominantly exterior perforated screen constructed from bricks, sandstone, laterite, and khondalite—by incorporating MBC. Jaali has historically been used to cool incoming air through its intricate patterns, drawing inspiration from the unique architectural styles that prevailed in India during the 16th to 18th centuries [31]. The Jaali's mechanism relies on filtering solar radiation, promoting controlled airflow, and facilitating evaporative cooling. Previous simulation studies have sought to quantify and optimise the performance of these screens. Research has shown that optimised jaali (and similar vernacular perforated screens such as 'Mashrabiya') geometry can yield significant energy savings, ranging from 6 to 26% [32,33] through optimised porosity and design. These findings underscore the effectiveness of this vernacular technique, establishing it as a highly efficient foundation for contemporary facade innovation.

The urgent pursuit of net-zero emissions in a warming world presents a significant opportunity to explore innovative solutions in the construction sector. Mycelium-based composites (MBCs) are emerging as a promising avenue for creating bio-based building materials with beneficial properties, including thermal insulation [34], acoustic absorption [35], fire-resistant properties [36], low embodied carbon [37], with the potential to utilise locally available waste materials [38] and local, low-energy production processes. Thus, bio-based materials such as MBCs may help achieve the World Green Building Council's 2030 vision, which aims to have all new buildings, infrastructure, and renovations have at least 40% less embodied carbon, with significant upfront carbon reduction, and all new buildings achieve net-zero operational carbon [39]. MBCs, characterised by their biodegradability and circularity, are viable alternatives to conventional high-embodied building insulation materials, such as extruded polystyrene foam, which has a degradation period of approximately 500 years in landfills. By combining lignocellulosic fibres with fungal mycelia, we can create a range of products, including biodegradable packaging [40], acoustic panels [41], interior design products [42], and sustainable alternatives to leather [43]. The cultivation of MBC involves propagating mycelia in fibrous substrates moulded into shapes, followed by heat treatment to halt further growth [24,26] or air-drying for large-scale applications to reduce embodied energy further [44]. The mechanical properties of these composites vary based on factors such as fungal species, substrate composition, and growing conditions [34,40,44,45], which opens up various avenues for research and development. Reported compressive strengths of MBCs range from 0.2–1.2 MPa for typical composites to over 2 MPa for high-strength 'mycocrete', while densities are generally 60–250 kg/m^3 depending on the substrate. By comparison, hempcrete exhibits compressive strengths of 0.3–0.9 MPa, whereas structural timber is much stronger, typically exceeding 40 MPa [44]. This positions MBCs as competitive with other lightweight bio-based materials for non-structural applications, while highlighting the need for further optimisation to expand their structural potential. The structural potential of MBC, which involves testing various bio-fabrication strategies such as bio-welding [46,47], reinforcement [48], blocks [49], and cladding for building applications and scaling up, has been explored; however, various limitations have been identified [50].

This study aimed to redesign the traditional 'jaali' by incorporating MBCs, a concept we term 'bio-jaali.' This approach aligns cultural heritage and vernacular architectural design with contemporary sustainability ethos by utilising a low-carbon, circular, bio-based material. This initiative preserves a valuable architectural tradition and enhances climate resilience in our built environment. This new design aims to improve passive ventilation while reducing indoor operative temperatures, making it particularly suitable for the extreme heat in New Delhi. To assess the effectiveness of the 'bio-jaali,' this study is one of the first (compared to the previous studies mentioned previously) to combine: 1) bio-fabrication of MBCs, 2) experimental cyclic humidity testing (for evaporative cooling potential), and 3) building-scale dynamic simulation of a façade element (bio-jaali) in an extreme climate of a megacity in a developing economy. Through these methods, the study explores the potential of integrating traditional architectural elements with modern sustainable materials, ultimately contributing to a more comfortable and energy-efficient indoor environment in a warming world.

2. Methodology

In this study, we focused on the temperate climate in New Delhi, India. The study consisted of three parts: (a) heat stress analysis with climate data analytics, (b) development and simulation of Jaali scenarios with dynamic building simulation, and (c) lab-based bio-fabrication and hygrothermal characterisation of MBC samples. Firstly, New Delhi's climate data for 1991–2019 were analysed to investigate the prevalence of heat stress using Equations (1) and (2). Secondly, we developed a building physics model of a 100 m2 indoor space in DesignBuilder. Then, 31 scenarios were assessed in the EnergyPlus simulation environment to determine the effect of different building screens on indoor operative temperature. EnergyPlus has been used in numerous studies on building physics and thermal comfort [51–55], which motivated our use of the simulation environment. Although several studies have reported the hydrophilic properties of MBCs [16], the literature lacks a clear understanding of their cyclic humidity-responsive behaviour, which cannot be accurately simulated using dynamic building simulation tools. Therefore, in the third part, we examined the cyclic moisture-responsive characteristics of MBC in the lab using bio-fabricated samples to enhance the evaporative cooling potential of the exterior building skin.

2.1. Heat stress analysis

We obtained 28 years of weather data (1991–2019) from the Meteoblue database (www.meteoblue.com) for the Heat Index (HI) analysis of New Delhi. The ambient temperature and relative humidity data were used to calculate the hourly heat index (HI) with the following Equation (1), adopted from [56]:

$$HI = -42.379 + 2.04901523T + 10.14333127R - 0.22475541TR - 6.83783 \times 10^{-3}T^2 - 5.481717 \times 10^{-2}R^2 + 1.22874 \times 10^{-3}T^2R + 8.5282 \times 10^{-4}TR^2 - 1.99 \times 10^{-6}T^2R^2 \quad (1)$$

where, T – Ambient dry bulb temperature (°F).

R – Relative humidity (integer percentage).

HI was selected for the study as it has been widely used in several studies to analyse the adverse effects of heat stress [57–60]. For the analysis in this study, we converted the ambient dry bulb temperature into °C with the following Equation (2), adopted from [61]:

$$C = 5/9(F - 32) \quad (2)$$

where, *C*- Ambient dry bulb temperature (°C).*F*- Ambient dry bulb temperature (°F).

Furthermore, we used the Heat Stress Index scale (Table 1) developed by the National Oceanic and Atmospheric Administration (NOAA) [62] to evaluate the HI for New Delhi.

2.2. Building physics modelling and simulation

A single-zone, naturally ventilated office space of 100 m^2 (10 m × 10 m × 3 m; Fig. 1) was modelled in DesignBuilder, with construction and materials as described in Table 2. These dimensions were selected to represent a typical medium-sized open office bay, striking a balance between realism (on an office scale) and computational feasibility, consistent with similar building energy simulation studies in the Indian context (e.g., jaali-screened façades in New Delhi libraries) [63]. The South façade was modelled as a fully glazed curtain wall to test a challenging scenario of maximal solar exposure, both to assess worst-case energy gain and because such glazed façades are increasingly used in modern office design in New Delhi (though often mitigated with shading devices) [63,64].

A jaali was modelled 0.32 m in front of the South façade (Fig. 1). The offset of 0.32 m was chosen because it is somewhat larger than the ~100 mm depth used in jaali optimisation studies in Delhi for visual/thermal comfort [63] providing additional separation to allow airflow, reduce direct heat transfer, and enable retrofit installation without significant structural changes. Given the computational time and limitations, the jaali design was kept simple, featuring a grid of square apertures, 0.07 m wide and spaced 0.07 m apart. The thickness of the jaali was denoted Th_s and varied across simulation scenarios. We used the 'generic office template' and 0.1110 people/m^2 for the activity template. Additionally, we utilised office equipment with a power density of 11.77 W/m^2. To eradicate the influence of other surfaces/walls apart from the curtain wall, adiabatic component blocks with 5 m width and 3 m height were created around the target zone (Fig. 1g).

Three temporal analyses were conducted to evaluate the impact of the bio-jaali on the indoor operative temperature. First, we analysed the effect annually. Secondly, we selected three summer dates (April 1, June 1, and August 1) and three winter dates (November 1, January 1, and March 1) to evaluate the impact on an hourly basis. We assessed outdoor and indoor operative temperatures against the India Model for Adaptive Comfort (IMAC), which suggested that the neutral temperature in naturally ventilated buildings varied from 19.6 to 28.5°C [65]. We also analysed the impact of stone and bio-jaali on the annual cooling demand across selected scenarios.

Table 1
Heat index and corresponding health impacts [62].

Heat Stress Index (°C)	Category	Dangers
27–32	Caution	Fatigue
32–41	Extreme caution	Sunstroke, heat cramps and heat exhaustion
41–54	Danger	Sunstroke, heat cramps, heat exhaustion, and even heat stroke
54+	Extreme danger	Heat/sunstroke

2.3. Scenario development

Depending on the objective, different scenarios were developed. In the base case, there was no jaali (Fig. 1e). Then, two types of jaali system were analysed – first one was the curtain wall with only the jaali (Fig. 1f) with hollow apertures around the sides, and the second type was a boxed jaali with no side apertures (Fig. 1h). For the study, the following scenarios, described in Table 3, were chosen to test the effect of the proposed bio-jaali on indoor operative temperature and cooling demand. Baseline scenarios were the no-jaali (BC) and sandstone jaali (SJ) on the south façade. When the jaali were box types, they were denoted with_Y at the end of the scenario name, such as SJ_Y and bio-jaali_1_Y. The other orientations were denoted as_E,_N, and_W for scenarios in which the curtain wall faced east, north, and west, respectively.

For the MBC material in the IDF file for EnergyPlus simulation, the conductivity, density, and specific heat properties were used for bio-jaali construction from [66]:

"Material, Mycelium material,
Rough,! - Roughness
Ths,! - Thickness {m}
0.069,! - Conductivity {w/m-K}
599,! - Density {kg/m3}
6894,! - Specific Heat {J/kg-K}
0.9,! - Thermal Emittance
0.6,! - Solar Absorptance
0.6;!- Visible Absorptance"

2.4. MBC samples and prototype bio-fabrication

The MBC samples and the prototype (of the modular panel of bio-jaali) were bio-fabricated with the following steps (Fig. 2A):

- **Preparation:** The 5 kg beechwood sawdust (substrate), with 99% of the granule size between 2 mm and 600 μm, was first placed into a large autoclavable filter bag for preparation (Fig. 2B (a)). Then, the substrate was hydrated with distilled water (5.5 kg). The filter bags were sealed with masking tape. Then, the filter bag was placed in an autoclave for 15 min at 121°C to sterilise the substrate. After autoclaving, the substrate-filled, sealed bags were examined (particularly in the masked-tape area for possible leaks, which can increase the risk of contaminating the substrates) while inside the autoclave to ensure there were no leaks. The autoclaved, sealed bag of substrates was removed from the autoclave and left to cool for 24 h on the lab table. The workspace was sterilised with a 70% Ethanol solution before starting from this stage to reduce the chance of contamination.
- **Inoculation:** After 24 h, the autoclaved filter bags were opened —near a Bunsen burner to maintain a sterile surrounding— to inoculate the substrate with 500 g (10% of the 5 kg substrate dry weight) *Ganoderma lucidum* (strain M9726), also known as Lingzhi or Reishi, grain spawn, which was purchased from Urban Farm-it (Kent, England). The species was conserved on a grain mixture at 4°C in a breathable Microsac 5 L bag (Sac O2 nv, Nevele, Belgium). We selected *G. lucidium* because it is an available, non-toxic fungal species in the UK and has been used in bio-fabricating MBC samples and prototypes in several studies due to its ability to colonise and grow rapidly on various biomass substrates containing lignin, cellulose, and hemicellulose [34,46,67], as well as resilience and antimicrobial properties [68], which reduces the probability of contamination.
- **Incubation_01:** After inoculation of the sawdust, the filter bags were sealed with masking tape and placed in a dark growth chamber at

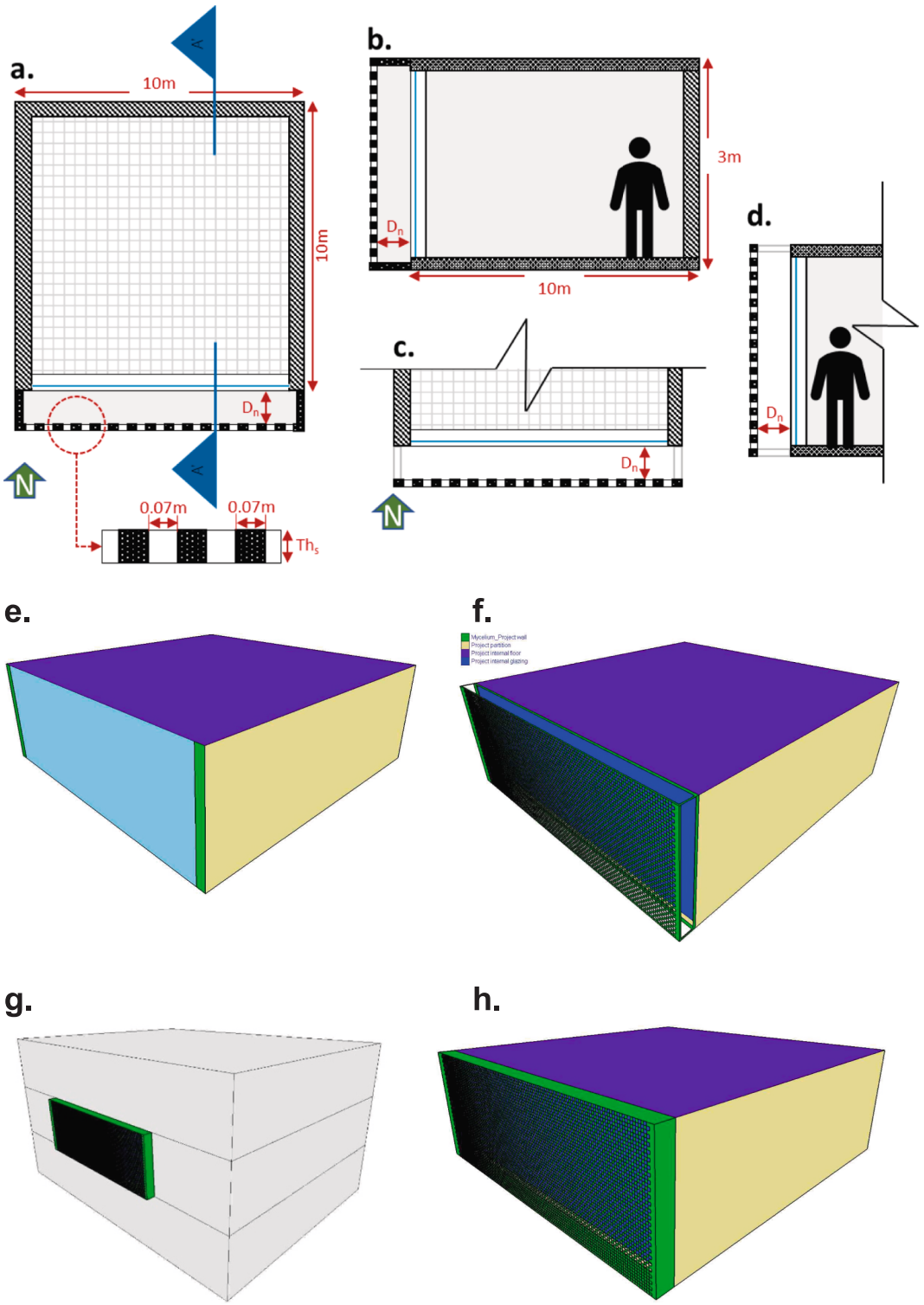

Fig. 1. (a) Plan of the indoor space for simulation (not to scale); Building physics model of (b, e) without Jaali and (c, f) with Jaali with apertures on other sides, (g, h) with boxed Jaali without apertures on other sides, developed in DesignBuilder (Version 7.0.2.006). In (g), the entire simulation setup is shown, where adiabatic component blocks with 5 m width and 3 m height were created around the target zone to eliminate the influence of other surfaces and walls except the curtain wall.

27°C. The inoculated filter bags were massaged daily for 7 days to break up clustered fungal colonies and spread them throughout the bags.

- **Moulding:** After seven days, the substrates were placed in custom-made mould trays for 70 mm (length) × 70 mm (width) × 30 mm (height) samples. Each tray could accommodate eight samples in two layers, as shown in Fig. 2B (c—e). The moulds were designed to fit inside the micro box with filtered lids, as shown in Fig. 2B (f).
- **Incubation_02:** The closed micro box with sample mould trays was placed in the growth chamber for five days.
- **Flipping:** After 5 days, the samples were inverted to improve oxygen access for mycelial growth on all surfaces. The inverted samples were then placed in the micro box (without the mould tray), with

Table 2
Construction name, thickness, and materials; for the material properties, we used a software database.

Name	Thickness (m)	Materials	U-Value (W/m^2-K)
Internal partition wall	0.150	Gypsum plasterboard (25 mm), airgap (10 mm), Gypsum plasterboard (25 mm)	1.639
External wall	0.233	Brickwork single-leaf construction light plaster	1.949
Internal floor	0.100	Cast concrete (Dense)	2.929
Internal ceiling	0.100	Cast concrete (Dense)	2.929
External glazing	0.019	Double-layer glazing with air gap and painted wooden frames	1.960

approximately 5–10 mm gaps between them to prevent bio-welding [46].

- **Incubation_03:** The closed micro box with inverted samples was placed in the growth chamber for an additional two days.
- **Post-processing:** 7 days after moulding and incubation, five samples were dried in an oven at 80°C for about 5 h to prevent further mycelial growth during post-processing. Similar post-processing was done after 11, 15, 19, 23 and 27 days of moulded incubation. The final samples were used for thickness and weight measurement, volume calculation and humidity responsivity testing.

Apart from the mould and incubation time, a similar bio-fabrication process was used for the prototype. For the prototype, a cylindrical plastic box was placed in the middle of the sterilised micro box, and the substrate was then poured into the box with dimensions of 160 mm (length), 160 mm (width), and 30 mm (height). The prototype was incubated for 13 days and then flipped. It remained incubated for 27 days before being post-processed (dried) in the oven.

2.5. Cyclic humidity responsiveness testing of MBC samples

The experimental work assessed the dimensional stability of MBC samples by examining their swelling, shrinkage, and recovery under varying humidity conditions. While the thermal properties of MBCs are well-documented in the literature [34], relatively little is known about their moisture-absorption behaviour and stability under fluctuating climatic conditions. For the bio-jaali concept, such stability is crucial, since excessive dimensional changes would complicate fabrication and long-term durability. The climate tests were therefore designed to evaluate how MBC responds to extreme-humidity scenarios and to determine whether its behaviour is compatible with conditions in New Delhi, where humidity levels are significantly higher at night and could contribute to evaporative cooling.

In this study, MBC samples from six different incubation times (7, 11, 15, 19, 23, and 27 days) were bio-fabricated and examined. Each incubation batch consisted of five samples measuring 70 mm wide, 70 mm long, and 30 mm thick. The goal was to determine which incubation duration shows the greatest humidity responsiveness. The experimental setup utilised a Memmert HPP IPP plus climate chamber, where the temperature was maintained at 25°C, with an average of 19.6–28.5°C within the thermal comfort range for India's office context [65], and the relative humidity (RH) alternated between two extreme levels: 10% and 90%. These specific settings were selected to assess the magnitude of moisture responsiveness in the MBC samples. The entire testing procedure was replicated eight times to observe the cyclic behaviour.

The cyclic tests lasted 32 consecutive days, with each cycle spanning four days. In the initial cycle, which commenced at RH = 90%, the materials were exposed to these conditions for two days. Weight, width, length, and thickness were measured hourly for the first 6 h, followed by

Table 3
Jaali materials and thickness for the base case and other scenarios.

Scenario	Objective	Jaali in front of a façade (Y/N)	Orientation of the curtain wall/jaali	Jaali material	Jaali distance from the curtain wall (D_n)	Jaali thickness (Th_s)
Base case (BC)	Baseline	N	South	–	–	–
BC_E		N	East	–	–	–
BC_W		N	West	–	–	–
BC_N		N	North	–	–	–
Sandstone Jaali (SJ)		Y	South	Sandstone	0.38 *m*	0.04 *m*
SJ_Y		Y	South	Sandstone	0.38 *m*	0.04 *m*
SJ_Y_E		Y	East	Sandstone	0.38 *m*	0.04 *m*
SJ_Y_W		Y	West	Sandstone	0.38 *m*	0.04 *m*
SJ_Y_N		Y	North	Sandstone	0.38 *m*	0.04 *m*
SJ_D1_Y		Y	South	Sandstone	0.15 *m*	0.04 *m*
SJ_D2_Y		Y	South	Sandstone	0.50 *m*	0.04 *m*
bio-jaali_1	Impact of thickness	Y	South	Mycelium	0.38 *m*	0.04 *m*
bio-jaali_2		Y	South	Mycelium	0.38 *m*	0.10 *m*
bio-jaali_3		Y	South	Mycelium	0.38 *m*	0.16 *m*
bio-jaali_4		Y	South	Mycelium	0.38 *m*	0.22 *m*
bio-jaali_{1D}1	Impact of distance	Y	South	Mycelium	0.15 *m*	0.04 *m*
bio-jaali_{1D}2		Y	South	Mycelium	0.50 *m*	0.04 *m*
bio-jaali_4_D1		Y	South	Mycelium	0.15 *m*	0.22 *m*
bio-jaali_4_D2		Y	South	Mycelium	0.50 *m*	0.22 *m*
bio-jaali_1_Y	Impact of side apertures	Y	South	Mycelium	0.38 *m*	0.04 *m*
bio-jaali_4_Y		Y	South	Mycelium	0.38 *m*	0.22 *m*
bio-jaali_{1D}1_Y		Y	South	Mycelium	0.15 *m*	0.04 *m*
bio-jaali_{1D}2_Y		Y	South	Mycelium	0.50 *m*	0.04 *m*
bio-jaali_4_D1_Y		Y	South	Mycelium	0.15 *m*	0.22 *m*
bio-jaali_4_D2_Y		Y	South	Mycelium	0.50 *m*	0.22 *m*
bio-jaali_1_Y_E	Impact of orientation	Y	East	Mycelium	0.38 *m*	0.04 *m*
bio-jaali_1_Y_W		Y	West	Mycelium	0.38 *m*	0.04 *m*
bio-jaali_1_Y_N		Y	North	Mycelium	0.38 *m*	0.04 *m*
bio-jaali_4_D2_Y_E		Y	East	Mycelium	0.50 *m*	0.22 *m*
bio-jaali_4_D2_Y_W		Y	West	Mycelium	0.50 *m*	0.22 *m*
bio-jaali_4_D2_Y_N		Y	North	Mycelium	0.50 *m*	0.22 *m*

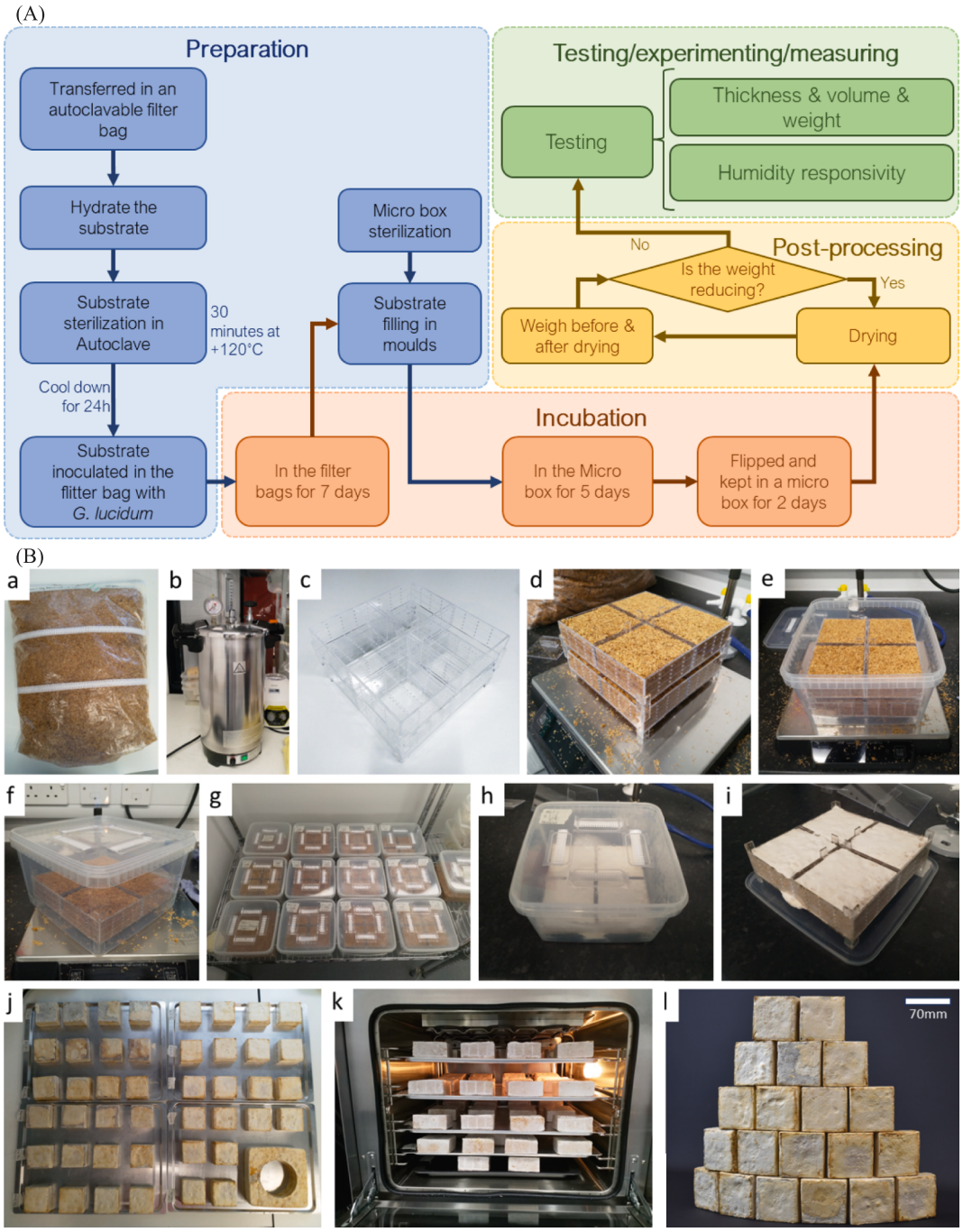

Fig. 2. (A) MBC samples and prototype bio-fabrication methodology; (B) Images of different steps of sample bio-fabrication — a) Beechwood substrate inside the filter bag, b) Autoclave, c) Custom-designed mould tray, e) Inoculated substrates in the mould trays, f & g) Micro box with mould tray filled with inoculated substrates, h) Micro boxes with samples on the shelves of the growth chamber, i) bio-fabricated samples in the moulds, j) the samples placed on the oven trays before drying them in the oven, k) Samples inside the oven for drying, and l) final samples —each sample with 70 mm (length) × 70 mm (width) × 30 mm (height)— stacked.

additional measurements at 24 and 48 h. After transitioning to a relative humidity (RH) of 10%, weight and dimensional measurements were recorded at 2-hour intervals for the first 6 h and then at 24 and 48 h. The first batch (5 samples) was incubated for 7 days and underwent 8 consecutive cycles of testing. Each subsequent incubation batch underwent one fewer cycle than the previous one. The analysis considered results from all successive cycles.

The dimensional and weight measurements were taken manually using an RS PRO Digital Calliper and a 50 g/0.001 g Milligram Precision Scale, respectively. The sample dimensions were measured in millimetres (mm) and collected simultaneously with the weight measurements. The dimensional and weight changes were calculated using Equation (3) adopted from [69]:

$$(Dimensional or Weight)change(\%) = \frac{D_{wet} - D_{dry}}{D_{dry}} \times 100\% \quad (3)$$

where: D_{wet} and D_{dry} represented the dimension/weight of a humid specimen (wet value) and its initial dimension/weight before exposure to moisture absorption (dry value), respectively. The results were reported as the mean of three different weight and dimensional mea-

surements for each sample.

3. Results

3.1. Heat stress in New Delhi

New Delhi's Heat Stress Index (HI) analysis (1991–2019) reveals a concerning shift toward more frequent and intense heat stress conditions (Fig. 3A–B). Hours in the caution level category have steadily declined over the past three decades, falling by more than 40% between 1991 and 2019, indicating that conditions are increasingly moving into higher stress categories. At the same time, extreme caution hours have remained persistently high, with only minimal reductions (around 1–3%) since 1991. Most concerning is the rapid growth of danger-level hours, which have increased by approximately 60% since 1991, reaching nearly 1,000 h in 2019, the highest recorded during this period. This escalation highlights an unprecedented intensification of heat stress risk in New Delhi, with potential implications for health, productivity, and building energy demand.

3.2. Dynamic building simulation

3.2.1. Indoor operative temperature: Annual

We simulated 31 scenarios for New Delhi's climate (Table 3). Overall, the results indicate that both sandstone jaali (SJ) and bio-jaali significantly improve indoor thermal conditions compared to the fully glazed base case. Annually, outdoor temperatures averaged 24.8°C (ranging from 6.5°C to 38.6°C). In contrast, the base case produced an exceptionally high mean indoor operative temperature of 41.8°C, with peaks above 51.0°C. Introducing an SJ reduced the mean to 33.6°C, while the bio-jaali (scenario 1) achieved a further reduction to 30.1°C. This represents a 3.5°C (approximately 10%) annual improvement in bio-jaali over sandstone.

Seasonal analysis underscores the same trend. In the summer months (April–September), outdoor temperatures averaged 30.6°C; yet, the base case yielded a mean indoor value of 42.8°C (Table 4). The SJ reduced this to 38.3°C, and the bio-jaali to 34.1°C—an 11% reduction relative to SJ. During winter (October–March), when outdoor conditions averaged 18.9°C, the base case maintained excessively high indoor levels (40.7°C). Both jaali types of substantially improved conditions, with the SJ reducing the mean to 28.8°C and the bio-jaali to 26.1°C (a further 9% reduction relative to the SJ).

Critically, while bio-jaali consistently delivered lower average, maximum, and minimum operative temperatures than sandstone in both summer and winter, the improvements were most pronounced during hot periods when overheating is most problematic. For example, summer peak indoor temperatures were approximately 13% lower with bio-jaali compared to sandstone, indicating a meaningful mitigation of extreme heat stress conditions (Fig. 4, Supplementary Fig. 1, and Supplementary Fig. 2).

After increasing the jaali thickness to 0.10 m, 0.16 m, and 0.22 m under the bio-jaali 2, 3, and 4 scenarios from 0.04 m for bio-jaali 1, the average indoor temperature increased to 30.3°C, 30.3°C, and 30.3°C, respectively (Fig. 4, Supplementary Fig. 1, and Supplementary Fig. 2). A 150% thickness increase in bio-jaali 2 resulted in an average indoor temperature increase of 0.14°C (+0.47%) compared to bio-jaali 1. Furthermore, 300% and 450% increases in jaali thickness also increased the average indoor temperature by 0.21°C (+0.69%) and 0.23°C (+0.75%), respectively, compared to bio-jaali 1. The average indoor operative temperature had a slight adverse impact on the thickness change in the bio-jaali.

To examine the impact of changing the distance of the jaali from the curtain wall, we simulated scenarios bio-jaali 1 (D1 and D2) and bio-jaali 4 (D1 and D2), where D1 and D2 were the distances of 0.15 m and 0.50 m, respectively, between the jaali and curtain wall, which was 0.38 m under bio-jaali 1. The results showed that the average indoor operative temperature was reduced to 29.57°C under bio-jaali 1_D1, which was 0.43°C lower than bio-jaali 1 (30.11°C). Under the bio-jaali 1_D2, the average annual indoor operative temperature increased to 30.07°C. In the case of bio-jaali 4_D1, the average indoor operative temperature increased to 29.36°C, which was 30.34°C under bio-jaali 4. However, the average operative temperature decreased to 30.42°C

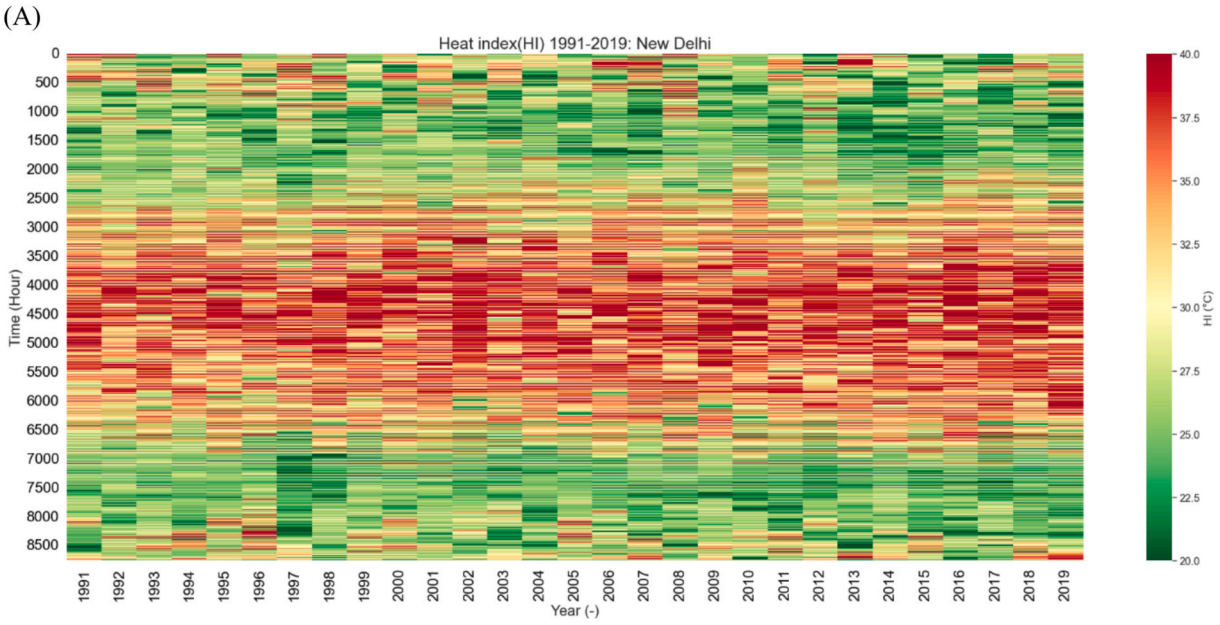

Fig. 3. (A) Heat Stress Index (HI) in New Delhi 1991–2019; (B) HI in 1995, 2001, 2005, 2011, 2015, and 2019. Here: ED = Extreme danger, D = Danger, EC = Extreme caution, C= Caution, and A = Acceptable. The prominent, recurring HI spikes observed at the beginning (January) and end (December) of several annual cycles (e.g., 1991, 1997, 2018, 2019) represent unseasonal heat-stress events. These are often attributed to anomalous atmospheric conditions during the typically cooler winter months, such as unusual shifts in wind patterns or the unseasonal intrusion of moist, warmer air masses (e.g., a delayed monsoon withdrawal or strong, moisture-bearing Western Disturbances). These phenomena temporarily raise both the ambient temperature and humidity, thus pushing the calculated Heat Index into the high 'Extreme Caution' or even 'Danger' categories.

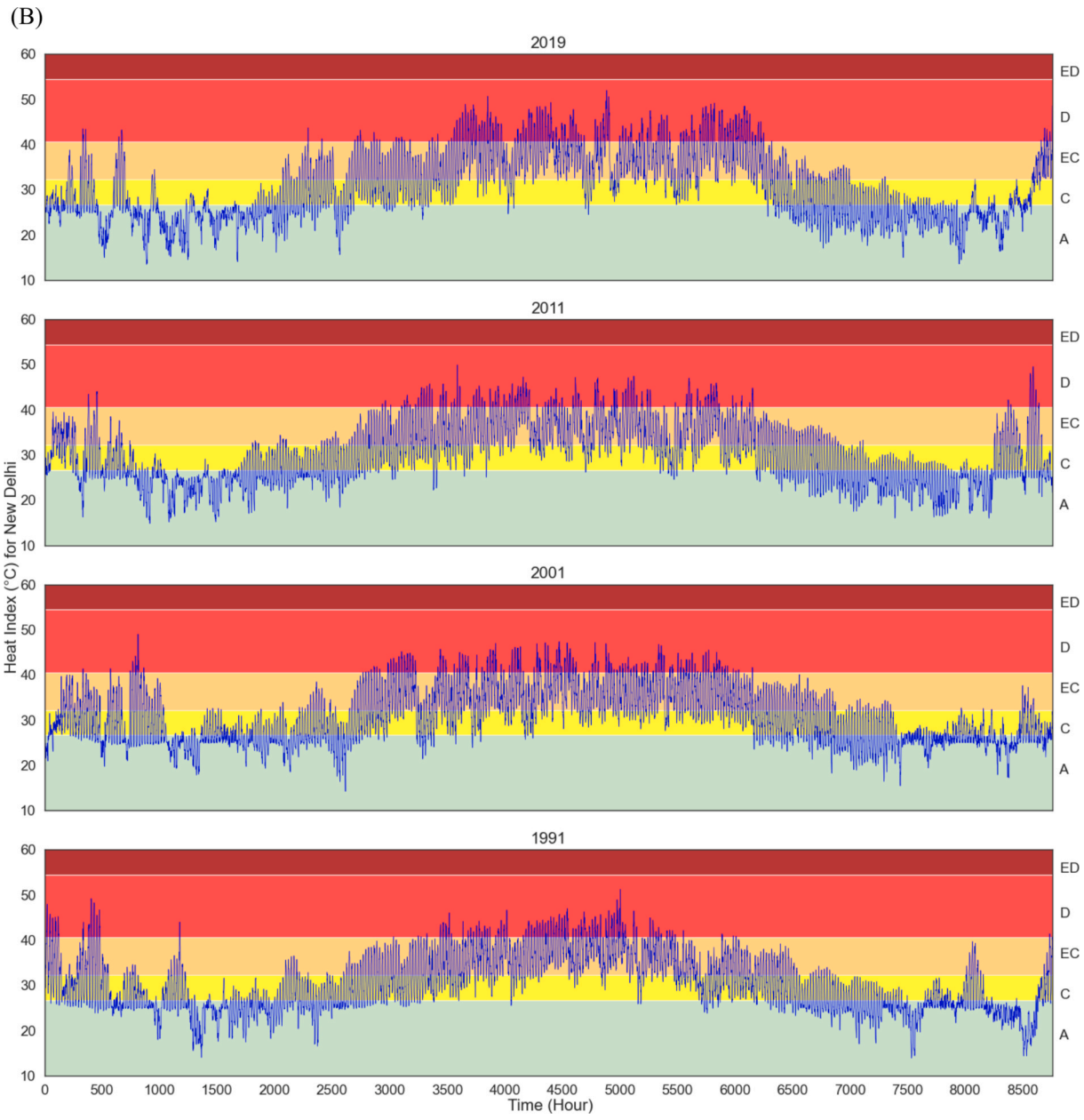

Fig. 3. (*continued*).

Table 4
Average indoor operative temperatures (°C) under different scenarios in New Delhi's climate.

Season	Outdoor Temp (Avg/ Min/Max)	Base Case (Avg/ Min/Max)	SJ (Avg/ Min/ Max)	Bio-jaali 1 (Avg/ Min/Max)	% Reduction (bio-jaali vs SJ)
Annual	24.8/6.5/ 38.6	41.8/ 25.6/51.0	33.6/ 18.0/ 45.3	30.1/ 18.7/42.1	~10% (avg)
Summer	30.6/21.9/ 38.6	42.8/ 34.4/50.7	38.3/ 30.1/ 45.3	34.1/ 25.5/42.1	11% (avg), 13% (max)
Winter	18.9/6.5/ 28.5	40.7/ 25.6/51.0	28.8/ 18.0/ 38.3	26.1/ 18.7/33.3	9% (avg), 13% (max)

under bio-jaali 4_D2. Therefore, the average indoor temperature increased when the jaali thickness was 0.04 m and the distance between the jaali and the curtain wall was reduced to 0.15 m. However, the indoor temperature increased when the jaali was thicker (0.22 m), and the distance between the jaali and the curtain wall was larger (0.50 m).

Several scenarios were developed and simulated to analyse the impact of side apertures (Fig. 1 and Table 3). The enclosed box-type scenarios were compared against the open jaali types with side apertures. In the case of the enclosed box-type sandstone jaali (SJ_Y), the average indoor operative temperature was reduced to 32.34°C, about 1.23°C lower than the SJ scenario. The average operative temperature reduced by 0.98°C under enclosed box-type mycelium-based jaali (bio-jaali 1_Y) compared to bio-jaali 1. Therefore, the enclosed box-type jaali (bio-jaali 1_Y and SJ_Y) performed better, further reducing indoor operative temperature, than bio-jaali 1 and SJ.

Regarding the jaali's orientation, we analysed the enclosed box-type jaali with sandstone and mycelium-based composite (which performed better than the jaali with side apertures) in comparison with the base

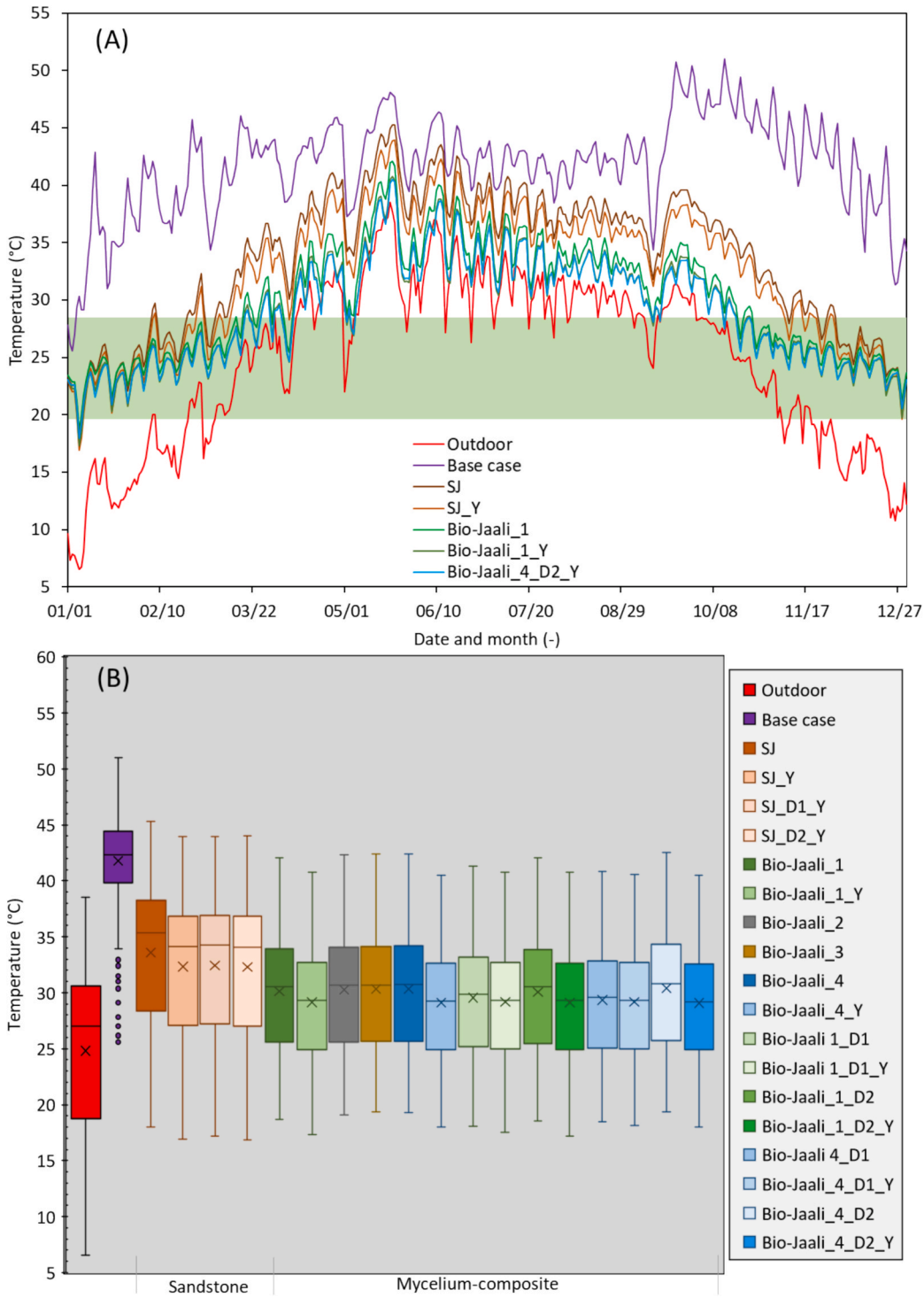

Fig. 4. (A) Daily outdoor and indoor operative temperature for a year under the base case, SJ, SJ_Y, bio-jaali 1, bio-jaali 4_D2_Y scenarios; and (B) Distribution and mean of daily outdoor and indoor operative temperatures for a year under the base case, SJ, SJ_Y, bio-jaali 1–4, bio-jaali 1 & 4 (D1 and D2), and bio-jaali 1 & 4 (D1 and D2)_Y scenarios. The rapid increase in Base Case operative temperature observed near the start of September (in A) is characteristic of New Delhi's post-monsoon climate. Following the monsoon's retreat, the combination of high solar radiation on clear days and high residual absolute humidity often leads to intense heat gain, causing a sharp rise in indoor temperature. Furthermore, this transition can be visually emphasised by the splicing methodology inherent in the Typical Meteorological Year (TMY) EPW file used for simulation.

case for east, north, and west, since all previous simulations were south-facing. Our results showed that for east orientation, SJ_Y_E and bio-jaali 1_E achieved average indoor operative temperatures of 31.99°C and 29.03°C, respectively, compared to the base case (BS_E) of 39.49°C. Similarly, regarding the west orientation, the average indoor operative temperature decreased to 32.12°C and 29.04°C under the SJ_Y_W and bio-jaali 1_W, respectively, compared to 40.83°C for BS_W. In the case of north orientation, BS_N showed that the average indoor operative temperature was 34.76°C, which decreased to 31.45°C and 21.83°C under SJ_Y_N and bio-jaali 1_N, respectively (Supplementary Fig. 3).

Our results showed that the bio-jaali outperformed the sandstone jaali in reducing the average indoor operative temperature during

summer and maintaining most winter days within the acceptable thermal comfort range (19.6–28.5°C) suggested by IMAC. However, this analysis did not reflect the bio-jaali's hourly impact on indoor temperature. To provide a comprehensive understanding, we meticulously analysed the effects of the jaali scenarios on hourly indoor temperatures on three selected summer and three winter days in the following sections.

3.2.2. *Indoor operative temperature: Summer days*

On 1 April, the beginning of the summer season, the average outdoor temperature was 28.84°C, with a maximum of 34.88°C in the afternoon and a minimum of 23.90°C at night. The initial period of summer was crucial for our analysis, as it sets the baseline for the subsequent days and helps us understand the impact of different Jaali scenarios on indoor temperature (Fig. 5). Under outdoor conditions, the base case scenario's average hourly indoor operative temperature was 40.04°C. This was significantly reduced under the influence of the sandstone jaali (SJ) and the enclosed box-type sandstone jaali (SJ_Y) to 35.31°C and 33.61°C, respectively. The average hourly operative temperature decreased to 30.67°C and 29.24°C under bio-jaali 1 and bio-jaali 1_Y (enclosed box-type MBC Jaali). This substantial reduction in the average hourly indoor operative temperature by 8.70–14.77°C under SJ, SJ_Y, bio-jaali 1 and bio-jaali 1_Y, compared to the base case, especially during the daytime, underscores the effectiveness of these Jaali scenarios. Even the enclosed box-type bio-jaali_4_D2_Y scenario, with increased thickness and spacing between the curtain wall and the Jaali, reduced the average hourly operative temperature to 29.05°C—only 0.19°C lower than bio-jaali_1_Y.

However, on 1 June, representing the peak and mid-summer periods, the average hourly outdoor temperature was 30.43°C, with a maximum of 34.45°C in the afternoon and a minimum of 24.13°C at night. The bio-jaali reduced the average indoor operative temperature from 43.16°C (Base case), 40.03°C (SJ) and 38.48°C (SJ_Y) to 34.73°C and 33.55°C under bio-jaali_1 and bio-jaali_1_Y, respectively. Under the Bio-

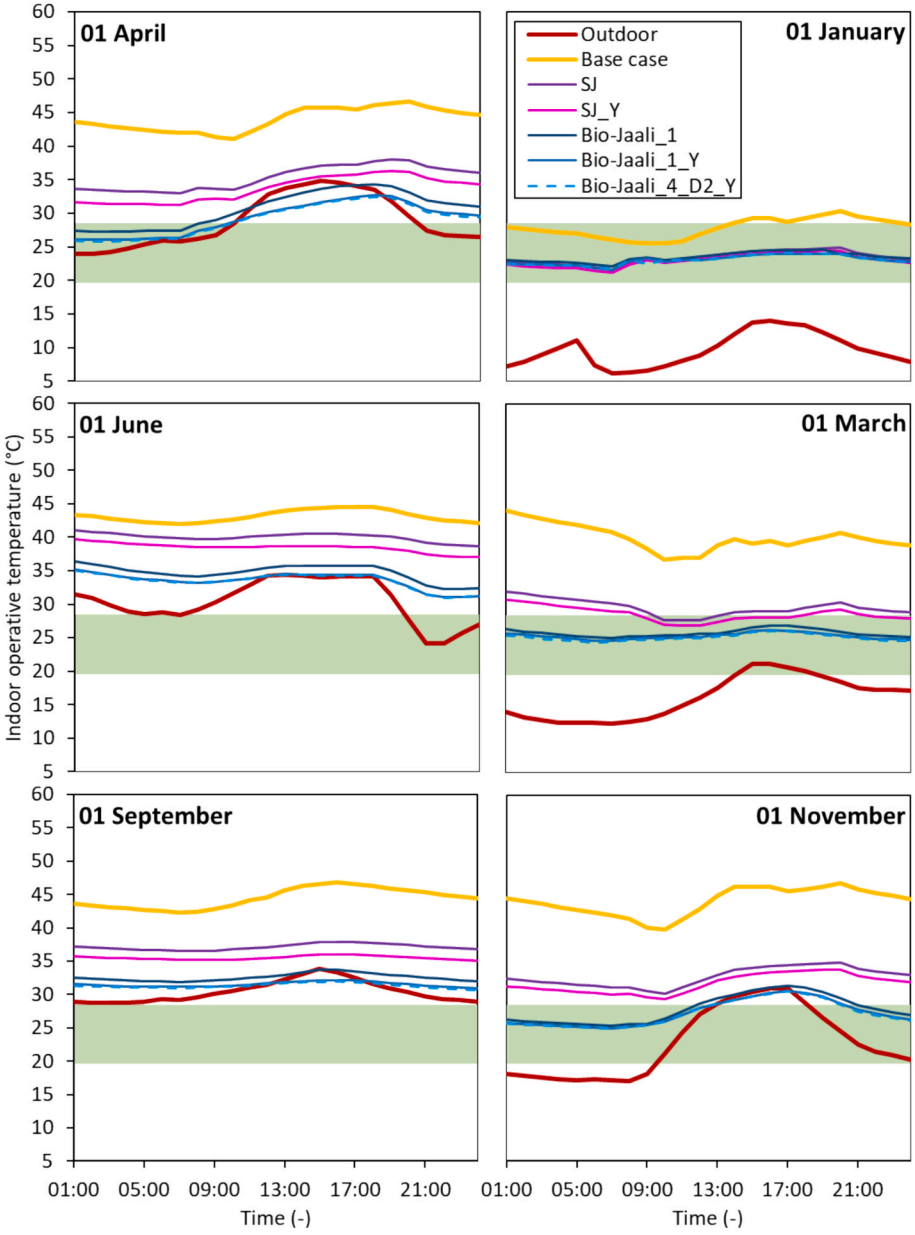

Fig. 5. Outdoor and indoor operative temperatures under the base case, SJ, bio-jaali 1, and 2 scenarios (the curtain wall or jaali facing south) on summer days (April 1, June 1, and September 1) and winter days (November 1, January 1, and March 1). The green area shows the acceptable (IMAC) thermal comfort temperature range. (For interpretation of the references to colour in this figure legend, the reader is referred to the web version of this article.)

Jaali_4_D2_Y scenario, the average hourly operative temperature decreased to 33.46°C, only a 0.09°C reduction from Bio-Jaali_1_Y. Although the indoor operative temperature was reduced with SJ and bio-jaali, it was never within an acceptable thermal comfort range on the summer days suggested by IMAC.

On 1 September, representing the end of summer, the average hourly outdoor temperature was 30.43°C, with a maximum of 33.80°C in the afternoon and a minimum of 28.73°C at night. Under the base-case scenario, the average indoor operative temperature was 44.46°C, with a maximum of 46.76°C and a minimum of 42.34°C. the average operative temperature was reduced to 37.14°C, 35.50°C, 32.57°C, 31.50°C, and 31.31°C under SJ, SJ_Y, bio-jaali_1, bio-jaali_1_Y and bio-jaali_4_D2_Y. Compared to the Base case and SJ, the operative temperature was reduced significantly by 12.96°C and 5.64°C under bio-jaali_4_D2_Y.

3.2.3. Indoor operative temperature: Winter days

On 1 November, the start of the winter season, the average hourly outdoor temperature was 22.72°C, with a maximum of 31.00°C in the afternoon and a minimum of 17.00°C at night (Fig. 5). The base case scenario's average hourly indoor operative temperature was 44.00°C. The average operative temperature was reduced to 32.66°C and 31.66°C under SJ and SJ_Y. Under bio-jaali_1, bio-jaali_1_Y and bio-jaali_4_D2_Y, the average operative temperature reduced to 27.83°C, 27.25°C and 27.18°C, respectively. Therefore, the indoor temperature decreased significantly by 11.35°C and 16.17°C compared to the outdoor base case under the SJ and bio-jaali_1 scenario. Under the box-type enclosed box-type SJ_Y, the average indoor operative temperature was reduced further by 1.00°C compared to SJ, and bio-jaali_1_Y and bio-jaali_4_D2_Y showed a reduction of 0.59°C and 0.66°C, respectively, compared to bio-jaali_1. Only the bio-jaali scenarios (bio-jaali, bio-jaali_1_Y, and bio-jaali_4_D2_Y) maintained the indoor operative temperature closest to the acceptable thermal comfort ranges during the day and within the acceptable range at night (maximum was 30.48–31.37°C, with the upper limit of IMAC at 28.5°C).

On 1 January, representing the peak and mid-period of winter, the average hourly outdoor temperature dropped to 9.64°C, with a maximum of 13.98°C in the afternoon and a minimum of 6.15°C at night. Under the SJ and SJ_Y scenarios, the average operative temperature was reduced to 23.38°C and 23.00°C, respectively, compared to 27.85°C in the Base case. The bio-jaali further reduced the average indoor operative temperature to 23.47°C, 23.04°C, and 23.04°C under the bio-jaali_1, bio-jaali_1_Y, and bio-jaali_4_D2_Y scenarios (Fig. 5). The SJ (SJ and SJ_Y) and bio-jaali scenarios (bio-jaali, bio-jaali_1_Y, and bio-jaali_4_D2_Y) maintained indoor operative temperatures within acceptable thermal comfort ranges throughout the day.

Moreover, on 1 March, marking the end of winter, the average hourly outdoor temperature was 16.16°C, with a maximum of 21.23°C in the afternoon and a minimum of 12.35°C at night. Under the base case scenario, the average indoor operative temperature was 40.04°C, which was reduced to 29.63°C, 28.63°C, 25.84°C, 25.37°C, and 25.17°C, respectively, under SJ, SJ_Y, bio-jaali_1, bio-jaali_1_Y and bio-jaali_4_D2_Y scenarios (Fig. 5). Among the SJ and bio-jaali scenarios, the indoor temperature remained within acceptable limits throughout the day (bio-jaali, bio-jaali_1_Y, and bio-jaali_4_D2_Y).

3.2.4. Cooling demand

The cooling demand analysis was conducted on the base case, SJ, SJ_Y, bio-jaali_1, bio-jaali_1_Y, and bio-jaali_4_D2_Y (Supplementary Fig. 4). Under the base-case air-conditioning (BC_AC) scenario, the annual cooling demand was 33.85 MWh. With the sandstone jaali on the south façade, cooling demand was reduced to 19.76 MWh, a 41.6% reduction compared to BC_AC. The annual cooling demand was further reduced by 5.3% (17.98 MWh) compared to BC_AC under the SJ_Y_AC scenario with box-type enclosed sandstone jaali. With the jaali constructed from MBC, the annual cooling demand was 20.35 MWh under bio-jaali_1, which was further reduced to 17.34 MWh under bio-jaali_1_Y, representing a 3.59% decrease compared to SJ_Y_AC. The lowest annual cooling demand of 16.78 MWh was achieved under bio-jaali_4_D2_Y, which is 50.44%, 15.09%, 17.55%, 6.68%, and 3.21% lower than the Base case, SJ, SJ_Y, bio-jaali_1, and bio-jaali_1_Y, respectively.

3.3. MBC's humidity responsiveness testing

Tests conducted across varying relative humidity levels (10%–90%–10%) demonstrated that MBC samples remained dimensionally stable, with changes in length, width, and thickness consistently below 3% across all batches and cycles (Fig. 6). This stability suggests that MBCs could be fabricated without the allowances for expansion and contraction typically required for wood.

Despite minimal dimensional changes, the MBC samples demonstrated a significant weight response to moisture. The highest observed weight change occurred in the 15-day incubation batch, reaching 17.2% on Day 2 of the second cycle (Fig. 7). Initially, the weight change increased gradually over the first three batches (7, 11, and 15 days of incubation), reaching 17% at 15 days, and then decreased steadily to 13% at 27 days of incubation. The response was fast, with the weight change at a humid state (90% RH) ranging between 12% and 17% within 24 h, depending on the incubation batch. In contrast, when exposed to a dry state (10% RH), the average weight change dropped to 0.5% within 24 h. The weight change exhibits a pattern in which the moisture absorption rate diminishes over time after the material is wet (Fig. 7). This indicates that MBC exhibits a higher absorption rate, which decreases after the first day. Similarly, MBCs exhibit nonlinear moisture release during drying, losing nearly 50% of the water they gain within the first 6 h. This rapid uptake and release of moisture highlight the potential of MBCs for evaporative cooling applications, particularly in climates like New Delhi, where high night-time humidity could be exploited for passive cooling.

Compared to natural fibrous materials, MBC demonstrated a greater absorption capacity than wood (approximately 12% swelling in response to moisture changes [70]) and comparable responsiveness to thin wood veneers, with reaction times on the order of minutes. While this suggests promise for bio-jaali applications, further studies on durability under prolonged outdoor exposure are needed, as external use would subject MBC to repeated wetting and drying cycles and potential biological degradation.

4. Discussion

4.1. Heat stress and the need for passive cooling

The reported heat stress index (HI) data in New Delhi between 1991 and 2019 reveal concerning trends. While the number of hours under the caution level has shown a significant reduction—by 43% compared to 1991 and similarly lower percentages relative to 2011 and 2015—the number of extreme caution hours has remained relatively static, with only a minimal decrease. More alarming, however, is the pronounced increase in hours classified as danger level; for example, the danger-level hours in 2019 (974 h) represent a 60% increase compared to 1991. This upward trend in danger-level exposure implied that, despite some mitigation at lower threshold levels, New Delhi's climate became increasingly hostile during peak heat events, which also increased their frequency. This reinforces the urgency of scalable passive cooling strategies. While traditional sandstone jaali provides some mitigation, its limited thermal performance highlights the need for alternative façade materials that can both insulate and adaptively respond to humidity. This historical climatic variability (Fig. 3) underscores the critical need for an adaptive façade, such as the bio-jaali, that can respond not only to peak summer heat but also to intermittent, unseasonal thermal stress.

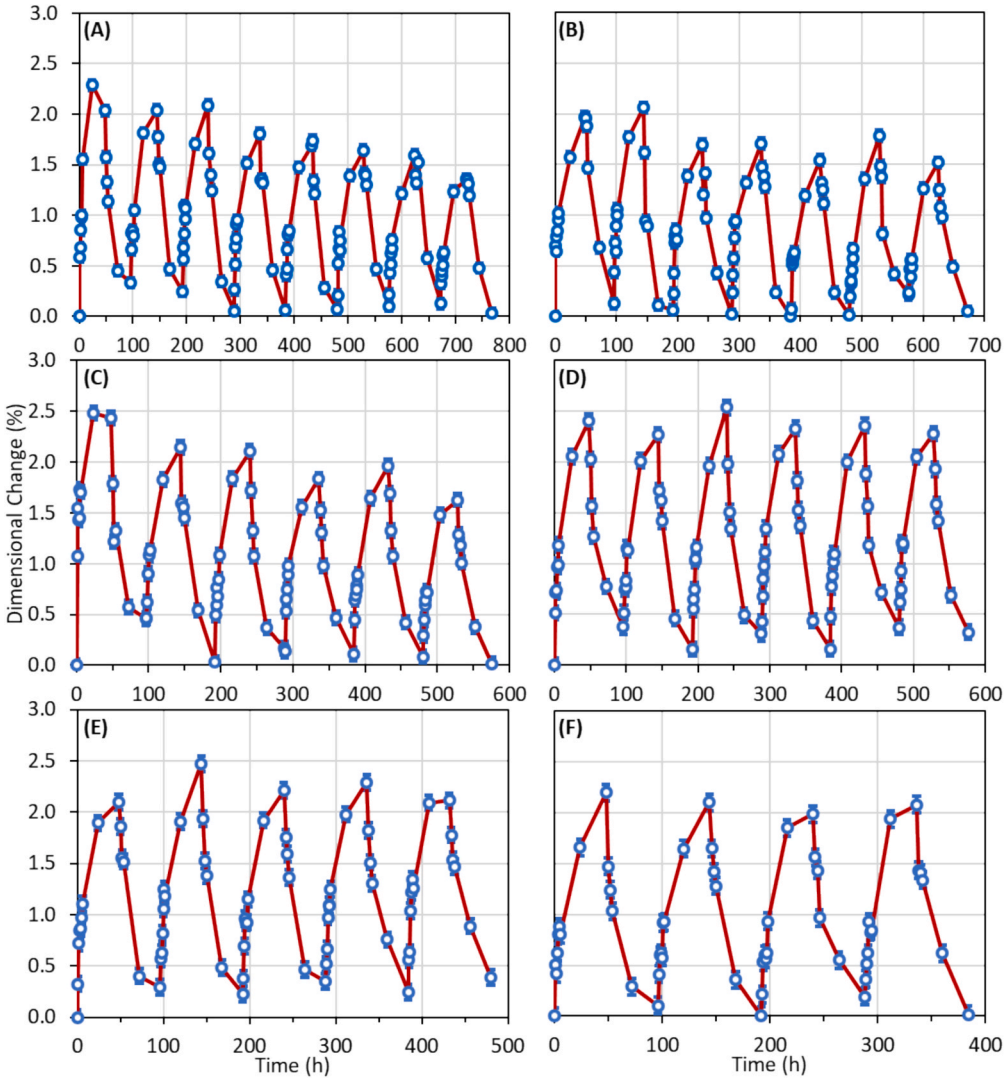

Fig. 6. Cyclic tests on the moisture responsiveness of MBC samples with (A) 7, (B) 11, (C) 15, (D) 19, (E) 23 and (F) 27 days of incubation, measuring the dimensional change (%) over time (h) at a constant temperature (T = 25℃) and two different relative humidity (RH) levels (10%—90%).

4.2. Performance of bio-jaali vs. conventional systems

The study analysed building envelope scenarios using jaali panels, comparing traditional sandstone jaali with bio-jaali. Dynamic building simulations showed that replacing sandstone with MBC could reduce the average annual indoor operative temperature by about 3.46°C (10% reduction). Given an average outdoor temperature of 24.81°C, with a maximum of 38.55°C, the base-case indoor temperature averaged 41.79°C. However, using bio-jaali_1 reduced the average temperature to 30.11°C, significantly improving thermal comfort and energy efficiency.

Seasonal analyses further demonstrated the variability in performance. During the summer, the base-case indoor operative temperature was high (e.g., 42.84°C on early-summer days), with reductions of up to 14.77°C achieved by deploying the bio-jaali configurations. Despite these improvements, we acknowledged that even the improved scenarios did not consistently keep indoor temperatures within the acceptable thermal comfort range defined by IMAC on peak summer days. In winter, however, the performance gains were even more pronounced. For instance, under bio-jaali scenarios, indoor temperatures were reduced to levels within or near the recommended comfort range, with the enclosed box-type variants (e.g., bio-jaali_1_Y) performing exceptionally well. The results suggested that while jaali systems made of MBC were highly effective under milder conditions, additional strategies, such as fans, air coolers, and even air-conditioning units, may be necessary to achieve comfort during extreme summer conditions.

4.3. Impact of jaali configuration and orientation

The study's exploration of varying jaali configurations—including modifications in thickness, distance from the curtain wall, and the presence of side apertures—provides a nuanced understanding of the interplay between design parameters and thermal performance. For instance, increasing the bio-jaali thickness generally led to a slight rise in the indoor operative temperature, likely because a thicker layer reduced the depth of shading perforations and limited cross-ventilation, thereby restricting heat dissipation. This suggests not only a trade-off between shading and airflow but also a potential limitation in the extent to which thickness alone can improve thermal performance. Adjustments to the distance between the bio-jaali and the curtain wall were also significant, reducing the gap to 0.15 m and enhancing shading effectiveness without severely impeding ventilation. The configuration that maintained the lowest indoor temperatures combined the thinnest tested bio-jaali panel (0.05 m) with this 0.15 m gap—conditions referred to here as 'minimal thickness' and 'optimised distance.' Beyond this point, further increases in thickness or additional changes in spacing produced negligible improvements, indicating a plateau effect that may reflect the diminishing

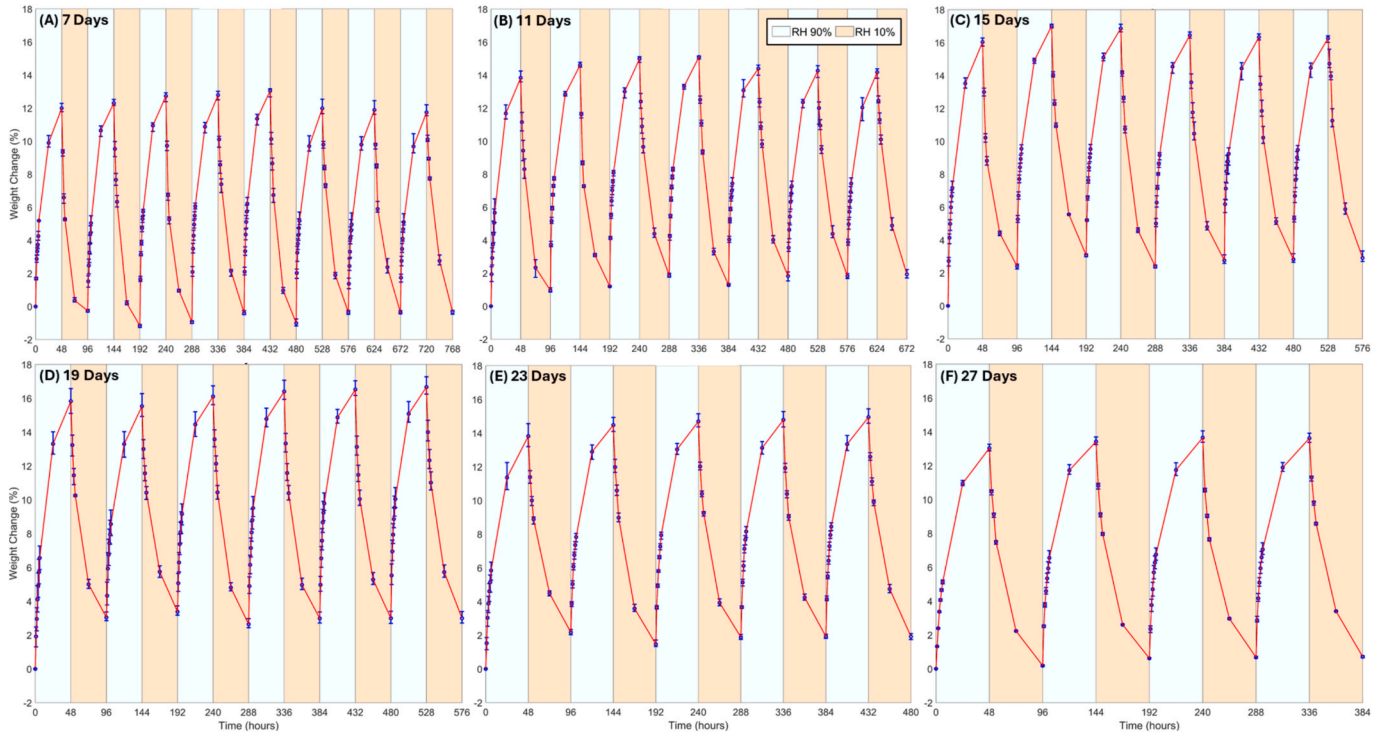

Fig. 7. Cyclic tests on MBC's moisture responsiveness of (A) 7, (B) 11, (C) 15, (D) 19, (E) 23 and (F) 27 days of incubation, measuring the weight change (%) over time (h) at a constant T = 25℃ and two different RH levels (10–90%).

influence of geometric modifications once a balance between shading and airflow has been achieved.

Additionally, the orientation of the jaali significantly influenced performance. In simulations for south, east, north, and west orientations, the enclosed box-type jaali configurations consistently reduced indoor operative temperatures compared to their base case counterparts (Supplementary Fig. 5, Supplementary Fig. 6, and Supplementary Fig. 7). For example, in the east-facing orientation, the bio-jaali variant reduced the average indoor temperature by more than 10°C relative to the base case. This directional sensitivity underscores the importance of tailored facade design strategies that account for solar exposure and local climatic conditions. It also reinforces that a one-size-fits-all approach may be less effective than a design optimised for the building's specific solar orientation and thermal load characteristics.

4.4. Cooling demand reductions

From an energy perspective, the cooling demand analysis further validates the efficacy of the jaali modifications. The base case scenario required 33.85 MWh of cooling annually, which was significantly reduced when sandstone or bio-jaali were used. The sandstone jaali alone achieved a 41.6% reduction, and further optimisation via an enclosed box-type configuration (SJ_Y_AC) yielded an additional reduction. However, the most impressive results were achieved with the MBC-made jaali configurations, particularly bio-jaali_4_D2_Y, which reduced the cooling demand by more than 50% compared to the base case. These reductions not only had the potential to improve occupant comfort but also translated into considerable energy savings and reduced carbon emissions—a critical consideration in sustainable architecture for rapidly warming climates.

4.5. Moisture responsiveness of MBC: Potential of evaporative cooling

The lab-based cyclic tests revealed minimal dimensional changes (<3%) across repeated cycles at various relative humidity levels, demonstrating that the MBC remains dimensionally stable under fluctuating moisture conditions. However, the material exhibited a significant weight change, with the most tremendous change observed in the 15-day incubation batch, reaching 17.2% on Day 2 of the cycle. The highest weight change might be the result of the densest mycelial networks in the sawdust substrate for samples with moulded incubation of 11–15 days (Supplementary Fig. 8). The rapid moisture absorption and non-linear drying characteristics indicate that MBC responds quickly to changes in humidity. This feature could be advantageous in passive building skin design strategies, such as evaporative cooling. Nevertheless, while the rapid responsiveness was promising, the non-linear behaviour and potential long-term effects of cyclic moisture exposure on material durability require further investigation.

Our preliminary bio-fabricated MBC samples (Supplementary Fig. 8) and prototype panel (Fig. 8) exhibited strong hydrophilic behaviour under high relative humidity conditions, consistent with trends reported in the literature for MBCs [34]. In our tests, the moisture uptake was at the lower end of the published ranges, which may be attributed to differences in substrate type, incubation time, or fabrication method. While high moisture absorption enhances responsiveness to humidity, enabling potential applications in evaporative cooling, it also poses durability challenges. Previous studies suggest that outdoor-exposed MBC panels may degrade within approximately 7–8 months [71], though this timescale is highly dependent on environmental exposure, climate zone, and substrate composition. Since decomposition is often linked to the biodegradability of lignocellulosic substrates, the use of denser substrates, such as hardwood sawdust, may extend service life and warrants further investigation.

The low mechanical strength and limited durability of MBCs remain critical barriers to their broader application, especially in external building components. Nevertheless, the bio-fabrication process enables the creation of lightweight, perforated forms that can serve as shading or ventilated screen systems. Compared to conventional materials for jaali, such as stone or timber, MBC panels are substantially lighter: 241 kg/m^3 for the MBC bio-jaali prototype compared to ~ 600–900 kg/m^3 for wood such as oak [72] and more than 2000 kg/m^3 for sandstone [73], offering advantages in handling and installation. Unlike timber, which can also

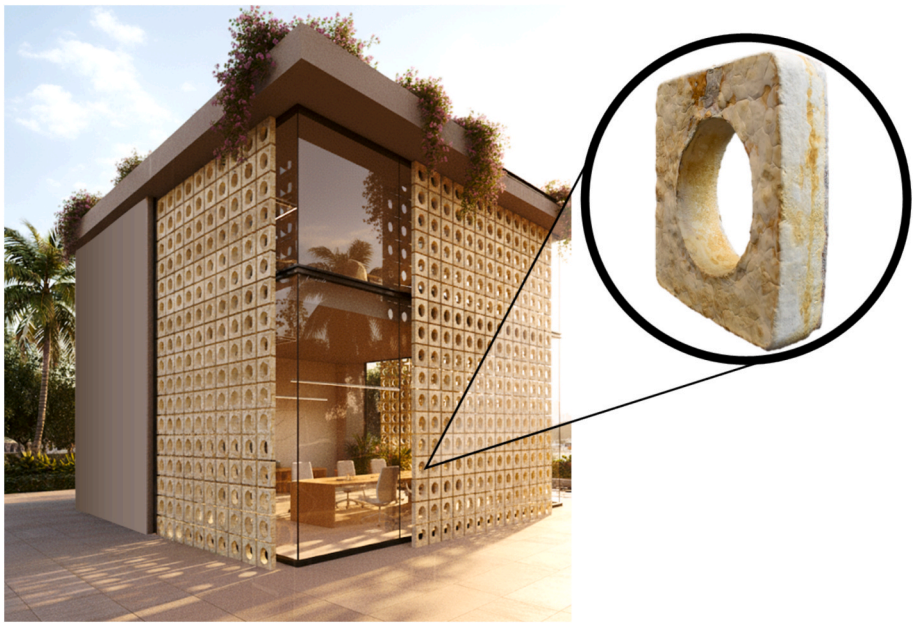

Fig. 8. Bio-fabricated 160 mm × 160 mm bio-jaali prototype panel with circular aperture. The building is a conceptual design showing the potential application of the prototype module.

be perforated for jaali, MBCs provide additional benefits, including their potential for passive evaporative cooling through humidity responsiveness and their low embodied energy and compostable end-of-life profile. However, these advantages must be balanced against the current limitations of rapid moisture-driven degradation, which future research should address through substrate optimisation, surface treatments, or hybridisation strategies.

While intrinsic thermal conductivity was outside the scope of this study, the heat stress properties of the bio-jaali were leveraged through two primary mechanisms: density reduction and hygrothermal performance. Compared to the conventional sandstone jaali (a high-density, high-thermal-mass solution), the MBC offers significantly lower density, resulting in a low-embodied-energy facade. This lightweight nature is competitive with other bio-based composites such as hempcrete and wood fibre, but the critical distinction lies in the dynamic, moisture-driven cooling.

Regarding moisture absorption, which is key to the bio-jaali's passive cooling strategy, the developed MBC demonstrates a unique advantage. Compared with other biodegradable materials, the MBC exhibits a high water-retention capacity (up to 17.2% weight gain), which is essential for evaporative cooling, without the typical drawback of hygrothermal degradation. Our results showed the material maintained dimensional stability (<3% change) across repeated wetting and drying cycles. This combination of high absorption and high stability is the critical difference, ensuring durability and consistent performance in a fluctuating climate where moisture-responsive facades must resist repeated swelling and shrinkage.

Beyond building-level performance, this study provides new evidence of the cyclic humidity responsiveness of MBCs. The composites remained dimensionally stable but rapidly absorbed and released moisture (up to a 17.2% change in weight within 48 h). This characteristic introduces the possibility of evaporative cooling, a function not observed in stone or timber jaali. By experimentally demonstrating this dual role—thermal insulation plus moisture-driven adaptability—we advance the understanding of MBCs as dynamic façade materials rather than static insulators.

4.6. Implications, limitations, and future directions

A. Research significance and comparative performance

The significant difference between this study and previous research on MBCs is the focus on dynamic, building-scale performance. Prior work primarily established static material properties for insulation. Our study uniquely extends this by:

- Validating the MBC's dynamic, cyclic hygrothermal performance for evaporative cooling in the lab.
- Integrating this material into a full-scale architectural element (the Bio-jaali).
- Quantifying the resultant heat stress mitigation through dynamic building simulation, demonstrating tangible outcomes like the 14.8°C peak temperature reduction and 50.4% energy saving.

This integration provides the missing link for translating MBCs into a viable, climate-adaptive façade solution. The magnitude of the thermal benefits achieved is highly favourable when compared to similar modelling studies. Studies analysing conventional or optimised jaali and passive façade designs typically report cooling energy savings ranging from 6% [74] to 23% [75]. Our finding of a 50.4% reduction in cooling energy validates the innovative strategy of combining MBCs' superior hygroscopic properties with vernacular design principles.

B. Model robustness, limitations and future directions.

Our model, utilising dynamic simulation and integrating experimentally validated hygrothermal data, provided a robust framework. Strengths of the modelling approach include the high-resolution scenario analysis across varying jaali thicknesses and the use of integrated material properties. However, to guide future research, several limitations must be noted:

- **Climate data limitation:** The European Centre for Medium-Range Weather Forecasts (ECMWF) Reanalysis 5th Generation dataset was used in our climate analysis. However, the estimation process of the dataset involved certain assumptions, inaccuracies, and

uncertainties [76,77]. These factors introduce nuance and potential variability that could affect the accuracy and reliability of the results.

- **Methodological robustness:** The simulations, while comprehensive, were based on specific climatic conditions pertinent to New Delhi and a single building configuration. The generalisability of these findings to other climatic regions or building typologies remains an open question. Future work should consider a broader range of conditions and typologies to assess the robustness of the observed trends. More critically, the current simulation relies on simplified correlations to model complex, localised airflow and moisture dynamics through the jaali perforations, rather than on high-resolution Computational Fluid Dynamics (CFD). Future work should use CFD to refine the dynamics of heat, moisture and air movement through and around MBC.
- **Thermal comfort in extreme conditions:** Although the MBC building skin systems significantly reduce indoor temperatures, they do not always bring the operative temperature within the acceptable thermal comfort range during peak summer days. This indicates a potential need for hybrid solutions that combine facade modifications with other passive or active cooling strategies.
- **Fire resistance testing:** Fire resistance is a key parameter for building skin application for any material. Existing studies have shown that MBCs exhibit greater fire resistance with the *T. versicolor* species [36]. However, our study's scope was narrowly focused on thermal (cooling) and moisture (evaporative cooling) performance as a priority for the heat-stress challenge, with fire resistance testing secondary for this initial work. Further research should investigate the fire-protection capabilities of MBC derived from *G. lucidum*.
- **Material durability and lifecycle analysis:** While the rapid moisture response of MBC was beneficial for adaptability, it also raised questions about its long-term durability. Further research should investigate the lifecycle performance of these materials, encompassing not only life-cycle carbon and embodied carbon but also weather protection and enhancement of mechanical strength, as well as potential degradation under cyclic environmental stresses.
- **Energy and environmental impact:** The marked reductions in cooling demand were promising from an energy efficiency standpoint. However, a complete environmental impact assessment—including the embodied energy of producing MBCs and their overall carbon footprint—would provide a more holistic understanding of their sustainability credentials, which studies such as [37] examined but require further research.

C. Extended applications and global transferability.

The bio-jaali's demonstrated performance in a challenging climate suggests broad applicability beyond New Delhi. The dual functionality of the MBC—thermal buffering and hygroscopic evaporative cooling—makes the concept highly transferable:

- **Climatic regions:** The bio-jaali is particularly suited for hot and dry climates (e.g., the Middle East), where the MBC's high moisture retention capacity (17.2% weight gain) would maximise the evaporative cooling effect. It also serves as an effective shading and thermal buffer in temperate climates during intermittent heatwaves.
- **Building typologies:** The low-cost and bio-based nature of the solution makes it ideal for residential and educational facilities lacking active cooling access. For commercial buildings, it provides a dynamic, sustainable second-skin façade contributing to green building certifications.
- **Feasibility and comparative economics:** Despite the lack of cost modelling, the bio-jaali presents a highly favourable economic case against conventional solutions. Its material inputs rely on biomass waste, and the manufacturing process uses low-energy bio-fabrication, circumventing the high material and energy costs associated with quarrying or cement production. This process results in a minimal (and potentially carbon-negative) embodied footprint, offering significant life-cycle cost savings and a low-risk, scalable alternative to energy-intensive construction.
- **Climate resilience in the face of global warming:** The effectiveness of the bio-jaali is directly enhanced by the predicted trajectory of global warming. As extreme heat events intensify and become more frequent, the need for decentralised, non-mechanical cooling becomes paramount. The bio-jaali's passive operation, low embodied carbon, and proven ability to significantly reduce peak indoor temperatures (up to 14.8°C) make it an inherently climate-resilient solution. By decoupling cooling from the strained electrical grid and utilising circular, bio-based materials, this approach offers a critical adaptive strategy that reduces reliance on energy-intensive active cooling, thereby mitigating the feedback loop between increasing heat and increasing energy demand.

In summary, the bio-jaali represents a robust, climate-adaptive façade principle, demonstrating a path to reimagining vernacular wisdom through bio-based composites to create low-carbon, climate-adaptive, and circular façades.

5. Conclusion

This study demonstrated the feasibility of bio-jaali made with mycelium-based composite (MBC) as a climate-responsive, low-carbon building skin for hot urban environments, with reinterpretations of traditional perforated façades in New Delhi's climatic context. In this study, analysis of historical climate data showed a 60% increase in 'danger-level' heat-stress hours in New Delhi over the 28-year period (1991–2019). Under the elevated extreme climatic context, dynamic simulations confirmed that bio-jaali significantly reduced indoor operative temperatures and cooling demand, outperforming conventional sandstone jaali. Bio-jaali reduced peak temperature by up to 14.8°C and cut annual cooling energy demand by 50.4%. Laboratory experiments provided new evidence of MBCs' humidity responsiveness— while dimensionally stable (<3% change), the composites exhibited rapid moisture uptake (up to 17.2% weight gain) and release, suggesting an untapped potential for evaporative cooling.

The novelty of this work lies in combining vernacular design, advanced building simulation, and bio-based material bio-fabrication and characterisation to establish the performance of MBC-made façades at both material and building scales. At the same time, limitations remain—including outdoor durability, peak-summer comfort, and mechanical robustness—the results open new directions for hybrid passive-active cooling strategies, protective treatments to extend service life, and full-lifecycle environmental assessments.

By bridging cultural heritage and circular material innovation, bio-jaali demonstrates how bio-based building skins can reduce reliance on cooling, lower embodied carbon, and enhance resilience to intensifying urban heat stress. As such, it represents a step toward sustainable, adaptive façades that align architectural practice with climate imperatives.

CRediT authorship contribution statement

Kumar Biswajit Debnath: Writing – review & editing, Writing – original draft, Visualization, Validation, Software, Resources, Methodology, Investigation, Formal analysis, Data curation, Conceptualization. **Natalia Pynirtzi:** Writing – review & editing, Writing – original draft, Visualization, Methodology, Investigation, Formal analysis, Data curation, Conceptualization. **Jane Scott:** Writing – review & editing, Writing – original draft, Supervision, Project administration, Funding acquisition, Conceptualization. **Colin Davie:** Writing – review & editing, Writing – original draft, Supervision, Methodology, Investigation. **Ben Bridgens:** Writing – review & editing, Writing – original draft, Supervision, Resources, Project administration, Methodology, Investigation, Funding acquisition, Conceptualization.

Declaration of competing interest

The authors declare that they have no known competing financial interests or personal relationships that could have appeared to influence the work reported in this paper.

Acknowledgements

This research was carried out as part of the 'RESPIRE: Passive, Responsive, Variable Porosity Building Skins' project (ID/Ref: 91782), which is funded by the Leverhulme Trust (https://www.leverhulme.ac.uk). We thank Meteoblue (www.meteoblue.com) for their collaboration on climate data. This work was also supported by the Chancellor's Research Fellowship (CRF), funded by the University of Technology Sydney (UTS).

Appendix A. Supplementary data

Supplementary data to this article can be found online at https://doi.org/10.1016/j.enbuild.2026.117104.

Data availability

The authors do not have permission to share data.

References

[1] UN, "The World's Cities in 2018—Data Booklet," United Nations, 2018.
[2] IPCC, "Climate Change 2022: Impacts, Adaptation, and Vulnerability," Cambridge University Press, 2022.
[3] K.B. Debnath, D. Jenkins, S. Patidar, A.D. Peacock, B. Bridgens, Climate change, extreme heat, and South Asian megacities: impact of heat stress on inhabitants and their productivity, ASME J. Eng. Sustain. Buildings Cities 4 (4) (2023) 041006.
[4] NIH, "Effects of Heat," National Institute of Environmental Health Sciences, 2022. [Online]. Available: https://www.niehs.nih.gov/research/programs/climatechange/health_impacts/heat/index.cfm#:~:text=Prolonged%20exposure%20to%20extreme%20heat,%2C%20cerebral%2C%20and%20cardiovascular%20diseases.. [Accessed 21 March 2022].
[5] K.B. Debnath, D.P. Jenkins, S. Patidar, A.D. Peacock, Understanding residential occupant cooling behaviour through electricity consumption in warm-humid climate, Buildings 10 (4) (2020) 78.
[6] K.B. Debnath, O. Osunmuyiwa, D.P. Jenkins, A.D. Peacock, A mixed-methods approach for evaluating the influence of residential practices for thermal comfort on electricity consumption in auroville, India, Electricity 5 (1) (2024) 112–133.
[7] GoI, "India Energy Security Scenarios 2047," Government of India, 2015. [Online]. Available: http://iess2047.gov.in.
[8] IEA, "Energy Efficiency: Cooling," International Energy Agency, 2019. [Online]. Available: https://www.iea.org/topics/energyefficiency/buildings/cooling/. [Accessed 21 March 2022].
[9] Y. Zhang, H. Qi, Y. Zhou, Z. Zhang, X. Wang, Exploring the impact of a district sharing strategy on application capacity and carbon emissions for heating and cooling with GSHP systems, Appl. Sci. 10 (16) (2020) 5543.
[10] X. Yan, Q. Men, Q. Meng, K.B. Debnath, Dual-stage collaborative optimal allocation of cooling source in ice storage air-conditioning systems considering daily and emergency demand response, Energy Buildings (2025) 116247.
[11] Y. Wei, J. Fan, Q. Meng, K.B. Debnath, Y. Yang, J. Liu, Y. Lei, EOLD: a reinforcement learning-based energy-optimised load disaggregation framework for demand-side energy management, Renew. Energy 252 (2025) 123536.
[12] Z.S. Zomorodian, M. Tahsildoost, Energy and carbon analysis of double skin façades in the hot and dry climate, J. Clean. Prod. 197 (2018) 85–96.
[13] S. Fantucci, V. Serra, C. Carbonaro, An experimental sensitivity analysis on the summer thermal performance of an Opaque Ventilated Façade, Energy Buildings 225 (2020) 110354.
[14] F. Yousefi, F. Nocera, The role of Ab-anbars in the vernacular architecture of iran with emphasis on the performance of wind-catchers in hot and dry climates, Heritage 4 (4) (2021) 3987–4000.
[15] A. Kaihoul, L. Sriti, K. Amraoui, S. Di Turi, F. Ruggiero, The effect of climate-responsive design on thermal and energy performance: a simulation based study in the hot-dry Algerian South region, J. Building Eng. 43 (2021) 103023.
[16] Y. Hui, Y. Tang, Q. Yang, A. Mochida, Numerical study on influence of surface vegetation on aerodynamics of high-rise buildings, Sustainable Cities Soc. 107 (2024) 105407.
[17] H.S.M. Shahin, Adaptive building envelopes of multistory buildings as an example of high performance building skins, Alexandria Eng. J. 58 (1) (2019) 345–352.
[18] R. Panchalingam, K.C. Chan, A state-of-the-art review on artificial intelligence for smart buildings, Intelli. Buildings Int. 13 (4) (2021) 203–226.
[19] K. Ma, Y. Yu, B. Yang, J. Yang, Demand-side energy management considering price oscillations for residential building heating and ventilation systems, IEEE Trans. Ind. Info. 15 (8) (2019) 4742–4752.
[20] X. Wang, X. Hu, Z. Liu, C. Zhu, R. Shen, B. Quan, X. Yan, W. Wang, X. Lu, J. Qu, Interpenetrating double-network ANF/MXene-K+ aerogels enable integrated electromagnetic interference shielding, infrared camouflage, and Joule heating in adaptive multifunctional systems, Nano Res. 18 (8) (2025) 94907702.
[21] J.H. Lee, M.J. Ostwald, M.J. Kim, Characterizing smart environments as interactive and collective platforms: a review of the key behaviors of responsive architecture, Sensors 21 (10) (2021) 3417.
[22] M. Sobczyk, S. Wiesenhütter, J.R. Noennig, T. Wallmersperger, Smart materials in architecture for actuator and sensor applications: a review, J. Intelli. Mater. Syst. Struct. 33 (3) (2022) 379–399.
[23] Y. Li, H. Li, R. Miao, H. Qi, Y. Zhang, Energy-environment-economy (3E) analysis of the performance of introducing photovoltaic and energy storage systems into residential buildings: a case study in Shenzhen, China, Sustainability 15 (11) (2023) 9007.
[24] Y. Shang, F. Tariku, Hempcrete building performance in mild and cold climates: Integrated analysis of carbon footprint, energy, and indoor thermal and moisture buffering, Building Environ. Elsevier 206 (2021) 108377.
[25] S. Balti, C. Maalouf, T. Moussa, G. Polidori, VC bio-hygrothermal and energy performances of earthen-based envelopes toward zero-carbon buildings: a case study from the Grand Est region, France, Energy Buildings, Elsevier (2025) 116563.
[26] X. Zhang, S. Wang, X. Chen, Z. Cui, X. Li, Y. Zhou, H. Wang, R. Sun, Q. Wang, Bioinspired flexible kevlar/hydrogel composites with antipuncture and strain-sensing properties for personal protective equipment, ACS Appl. Mater. Interfaces 16 (34) (2024) 45473–45486.
[27] Q. Long, G. Jiang, J. Zhou, D. Zhao, H. Yu, A cellulose ionogel with rubber-like stretchability for low-grade heat harvesting, Research 7 (2024) 0533.
[28] N. Lin, X. Luo, J. Wen, J. Fu, H. Zhang, K.H. Siddique, H. Feng, Y. Zhao, Black biodegradable mulching increases grain yield and net return while decreasing carbon footprint in rain-fed conditions of the Loess Plateau, Field Crops Res. 318 (2024) 109590.
[29] J. Zha, Z. Zhang, Reversible negative compressibility metamaterials inspired by Braess's paradox, Smart Mater. Struct. 33 (7) (2024) 075036.
[30] R. Prasad, R. Tandon, A. Verma, M. Sharma, N. Ajmera, Jaali a tool of sustainable architectural practice: understanding the feasibility and usage, Mater. Today: Proc. 60 (2022) 513–525.
[31] F.T. Azmi, "How India's lattice buildings cool without air con," BBC, 21 September 2022. [Online]. Available: https://www.bbc.com/future/article/20220920-how-indias-lattice-buildings-cool-without-air-con. [Accessed 14 September 2025].
[32] A. Ahmad, L. Bande, W. Ahmed, K. Tabet Aoul, M. Jha, Parametric optimization and assessment of modern heritage shading screen for a mid-rise building in arid climate: modernizing traditional designs, Buildings 15 (7) (2025) 1148.
[33] A. Taki, H. Kumari, Examining Mashrabiya's impact on energy efficiency and cultural aspects in Saudi Arabia, Sustainability 15 (13) (2023) 10131.
[34] M. Jones, A. Mautner, S. Luenco, A. Bismarck, S. John, Engineered mycelium composite construction materials from fungal biorefineries: a critical review, Mater. Design 187 (2020) 108397.
[35] M. Pelletier, G. Holt, J. Wanjura, L. Greetham, G. McIntyre, E. Bayer, J. Kaplan-Bie, Acoustic evaluation of mycological biopolymer, an all-natural closed cell foam alternative, Ind. Crops Prod. 139 (2019) 111533.
[36] M. Jones, T. Bhat, E. Kandare, A. Thomas, P. Joseph, C. Dekiwadia, R. Yuen, S. John, J. Ma, C.-H. Wang, Thermal degradation and fire properties of fungal mycelium and mycelium-biomass composite materials, Sci. Rep. 8 (1) (2018) 17583.
[37] A. Livne, H.A. Wösten, D. Pearlmutter, E. Gal, Fungal mycelium bio-composite acts as a CO2-sink building material with low embodied energy, ACS Sustainable Chem. Eng. 10 (37) (2022) 12099–12106.
[38] K. B. Debnath, C. Ton-That, N. Biloria and S, "Exploring the potential of Australian agricultural and industrial wastes from the source to bio-fabricating viable mycelium-based composites," in 4th International Conference of Sustainable Building Materials (ICSBM 2025), Eindhoven The Netherlands, 2025.
[39] WorldGBC, Bringing embodied carbon upfront: Coordinated action for the building and construction sector to tackle embodied carbon, World Green Building Council, London, 2019.
[40] E. César, G. Canche-Escamilla, L. Montoya, A. Ramos, S. Duarte-Aranda, V. M. Bandala, Characterization and physical properties of mycelium films obtained from wild fungi: natural materials for potential biotechnological applications, J. Polym. Environ. 29 (12) (2021) 4098–4105.
[41] N. Walter, B. Gürsoy, A study on the sound absorption properties of mycelium-based composites cultivated on waste paper-based substrates, Biomimetics 7 (3) (2022) 100.
[42] W. Sun, M. Tajvidi, C. Howell, C.G. Hunt, Insight into mycelium-lignocellulosic bio-composites: essential factors and properties, Compos. Part a: Appl. Sci. Manuf. 161 (2022) 107125.
[43] E. Elsacker, S. Vandelook, E. Peeters, Recent technological innovations in mycelium materials as leather substitutes: a patent review, Front. Bioeng. Biotechnol. 11 (2023) 1204861.
[44] R. Kaiser, B. Bridgens, E. Elsacker, J. Scott, BioKnit: development of mycelium paste for use with permanent textile formwork, Front. Bioeng. Biotechnol. 11 (2023) 1229693.
[45] J.K. Muiruri, J.C. Chuan Yeo, Q. Zhu, E. Ye, X.J. Loh, Z. Li, Sustainable mycelium-bound biocomposites: design strategies, materials properties, and emerging applications, ACS Sustainable Chem. Eng. 11 (18) (2023) 6801–6821.

[46] D. Raslan, E. Elsacker, K.B. Debnath, M. Dade-Robertson, The role of surface interventions in bio-welding mycelium based-composites, Sustainable Mater. Technol. (2025) e01326.
[47] B. Modanloo, A. Ghazvinian, M. Matini, E. Andaroodi, Tilted arch; implementation of additive manufacturing and bio-welding of mycelium-based composites, Biomimetics 6 (4) (2021) 68.
[48] E. Özdemir, A. Rossi, P. Eversmann, MycoCurva: stay-in-place fabric formworks for curved veneer-reinforced mycelium building components, Arch. Struct. Constr. 5 (1) (2025) 16.
[49] K. Joshi, M.K. Meher, K.M. Poluri, Fabrication and characterization of bioblocks from agricultural waste using fungal mycelium for renewable and sustainable applications, ACS Appl. Bio Mater. 3 (4) (2020) 1884–1892.
[50] S. Bitting, T. Derme, J. Lee, T. Van Mele, B. Dillenburger, P. Block, Challenges and opportunities in scaling up architectural applications of mycelium-based materials with digital fabrication, Biomimetics 7 (2) (2022) 44.
[51] X. Xu, J.E. Taylor, A.L. Pisello, Network synergy effect: establishing a synergy between building network and peer network energy conservation effects, Energy Buildings 68 (2014) 312–320.
[52] J.H. Yoon, R. Baldick, A. Novoselac, Dynamic demand response controller based on real-time retail price for residential buildings, IEEE Trans. Smart Grid (2014) 121–129.
[53] A. Al-janabi, M. Kavgic, A. Mohammadzadeh, A. Azzouz, Comparison of EnergyPlus and IES to model a complex university building using three scenarios: free-floating, ideal air load system, and detailed, J. Building Eng. 22 (2019) 262–280.
[54] S. Huang, D. Wu, Validation on aggregate flexibility from residential air conditioning systems for building-to-grid integration, Energy Buildings 200 (2019) 58–67.
[55] K.B. Debnath, D.P. Jenkins, "Simulation-based assessment of residential energy demand reduction strategies for cooling in a south Indian community," in Building Simulation and Optimization 2020, Loughborough, 2020.
[56] L.P. Rothfusz, N.S.R. Headquarters, The heat index equation (or, more than you ever wanted to know about heat index), National Oceanic and Atmospheric Administration, National Weather Service, Office of Meteorology, Fort Worth, Texas, 1990.
[57] M. Luo, N.-C. Lau, Characteristics of summer heat stress in China during 1979–2014: climatology and long-term trends, Clim. Dyn. 53 (9–10) (2019) 5375–5388.
[58] R. Modarres, M. Ghadami, S. Naderi, M. Naderi, Future heat stress arising from climate change on Iran's population health, Int. J. Biometeorol. 62 (7) (2018) 1275–1281.
[59] G. Choi, D.E. Lee, Changing human-sensible temperature in Korea under a warmer monsoon climate over the last 100 years, Int. J. Biometeorol. (2020) 1–10.
[60] S. Opitz-Stapleton, L. Sabbag, K. Hawley, P. Tran, L. Hoang, P.H. Nguyen, Heat index trends and climate change implications for occupational heat exposure in Da Nang, Vietnam, Clim. Services 2 (2016) 41–51.
[61] T.H. Fay, K.A. Hardie, Fahrenheit to Celsius: an exploration in college algebra, Math. Comp. Educ. 37 (2) (2003) 207–209.
[62] NWS, "What is Heat Index?," National Weather Service, 2020. [Online]. Available: https://www.weather.gov/ama/heatindex. [Accessed 2020].
[63] A. Rehman, A. Surapaneni, Multi-objective optimization of Indian jaali fenestration system for visual, thermal and perceptual performance using computational methods, Building Simul. (2021, 2021.).
[64] F. Tahmasbi, A.I. Khdair, G.A. Aburumman, M. Tahmasebi, N. Thi, M. Afrand, Energy-efficient building façades: a comprehensive review of innovative technologies and sustainable strategies, J. Building Eng. 99 (2025) 111643.
[65] S. Manu, Y. Shukla, R. Rawal, L.E. Thomas, R. De Dear, Field studies of thermal comfort across multiple climate zones for the subcontinent: India Model for Adaptive Comfort (IMAC), Building Environ. 98 (2016) 55–70.
[66] X. Zhang, J. Hu, X. Fan, X. Yu, Naturally grown mycelium-composite as sustainable building insulation materials, J. Clean. Prod. 342 (2022) 130784.
[67] D. Alemu, M. Tafesse, A.K. Mondal, Mycelium-based composite: the future sustainable biomaterial, Int. J. Biomater. 2022 (1) (2022) 8401528.
[68] S.M. Mousavi, S.A. Hashemi, A. Gholami, N. Omidifar, W.-H. Chiang, V.R. Neralla, K. Yousefi, M. Shokripour, Ganoderma lucidum methanolic extract as a potent phytoconstituent: characterization, in-vitro antimicrobial and cytotoxic activity, Sci. Rep. 13 (1) (2023) 17326.
[69] R.B. Hoadley, Understanding wood, Taunton press, Newtown, 2000.
[70] A. Holstov, B. Bridgens, G. Farmer, Hygromorphic materials for sustainable responsive architecture, Constr. Building Mater. 98 (2015) 570–582.
[71] T. Houette, B. Foresi, C. Maurer, P. Gruber, "Growing Myceliated Facades: Manufacturing and exposing experimental panels in a façade setting," in *Facade*, Tectonics (2020, 2020.).
[72] P.A. Tipler, G. Mosca, Physics for scientists and engineers, Macmillan, 2007.
[73] R.W. Young, R.A. Wray, A.R. Young, Sandstone landforms, Cambridge University Press, 2009.
[74] F. Alrashed, M. Asif, S. Burek, The role of vernacular construction techniques and materials for developing zero-energy homes in various desert climates, Buildings 7 (1) (2017) 17.
[75] H.M. Taleb, A.G. Antony, Assessing different glazing to achieve better lighting performance of office buildings in the United Arab Emirates (UAE), J. Building Eng. 28 (2020) 101034.
[76] ECMWF, "ERA5: data documentation," European Centre for Medium-Range Weather Forecasts, 30 October 2023. [Online]. Available: https://confluence.ecmwf.int/display/CKB/ERA5%3A+data+documentation#ERA5:datadocumentation-Accuracyanduncertainty. [Accessed 01 November 2023].
[77] ECMWF, "ERA5: uncertainty estimation," European Centre for Medium-Range Weather Forecasts, 05 May 2023. [Online]. Available: https://confluence.ecmwf.int/display/CKB/ERA5%3A+uncertainty+estimation#ERA5:uncertaintyestimation-(6)HowreliableistheERA5uncertaintyestimate?. [Accessed 01 November 2023].